8-24-2020 2:30 PM

Structural Performance of Ordinary and Laminated Glass during Fire Exposure

Amer Sabsabi, *The University of Western Ontario*

Supervisor: Youssef, Maged A., *The University of Western Ontario*

A thesis submitted in partial fulfillment of the requirements for the Master of Engineering Science degree in Civil and Environmental Engineering

Abstract

Façade and glazing elements constitute the skin of buildings. They are the interface between the inside and outside environment. Glass has low fire resistance and can quickly break during fire events. This creates new vents, which increase the oxygen supply and promote the flashover phenomenon. Existing methods for evaluating the structural fire safety of glass require expensive experimental tests or extensive knowledge of finite element (FE) modeling. This research provides simplified, rational, and reliable methods to assess the behavior of ordinary and laminated glass panels during fire exposure. The proposed methods provide the means to determine the glass temperature and its maximum thermal stress during fire exposure. These methods can be utilized by structural engineers, while designing buildings using performance-based design criteria.

Keywords

Façade; glass; laminated glass; fire exposure; thermal exposure; numerical modelling

Summary for Lay Audience

Façade and glazing elements are essential elements of any building, that provide a natural source of light and oxygen, while having high aesthetic value. These elements are mainly composed of glass, which has low fire resistance and can quickly break during fire events. This breakage increases the severity of the fire by creating a continuous supply of fresh oxygen. Therefore, it is crucial to address this issue by improving our understanding of glass behavior during fire events. Several types of glass products are available in the market. The two main types are ordinary and laminated glass panels. Ordinary glass is the one commonly used in buildings, while the laminated is composed of two glass panels with an interlayer in-between. This research investigates the problem of glass breakage during fire exposure and proposes simple yet reliable methods for engineers to ensure the safety of the building's occupants during fire exposure.

Co-Authorship Statement

This thesis has been prepared in accordance with the regulation for an Integrated-Article format thesis prepared by the Western University Graduate and Postgraduate studies. All numerical and analytical work presented in this thesis was performed by Amer Sabsabi. Work was reviewed by Prof. Maged Youssef and Dr. Salah El-Fitiany. Chapters 3 of this thesis has been submitted to a scholarly journal as a manuscript co-authored by Amer Sabsabi, Maged Youssef, Salah El-Fitiany, and Ajitanshu Vedrtnam. Professor Vedrtnam of Invertis University is the Indian collaborator for this project, which was funded by the NSERC Centres of Excellence: IC-IMPACTS (the India-Canada Centre for Innovative Multidisciplinary Partnerships to Accelerate Community Transformation and Sustainability). Chapter 4 will be submitted to a scholarly journal as a manuscript co-authored by Amer Sabsabi, Maged Youssef, Salah El-Fitiany, and Ajitanshu Vedrtnam.

Acknowledgments

I would first like to express my sincere gratitude to my advisor, Prof. Maged Youssef, for his guidance, patience, understanding and continued support throughout my master's studies. Prof. Youssef made sure that I worked in a stress-free, positive, cheerful work environment and provided all the support needed for me during my studies.

I would also like to express my greatest gratitude to Dr. Salah El-Fitiany for his continuous support and inspiration during this research. His help is greatly appreciated. My heartfelt appreciation also goes for my friends in Dr. Youssef's research group including Murad, Emad, Robert, Malek, and Mohamed Badr as they created a wonderful working environment throughout my MESc.

My thanks also go to my fellow graduate students for their continued friendship and enthusiasm and for making this experience enjoyable.

Above all, I would like to thank my family for all their support throughout my research and life.

Table of Contents

List of Tables

List of Figures

List of Abbreviations, Symbols, and Notations

b	Width of the frame (covered part of the glass)
Bi	Biot number
c	Glass' specific heat
c_{PVB}	PVB-Interlayer specific heat
$f_{t,PVB}$	PVB-Interlayer tensile strength
g	Gravitational acceleration
G_{PVB}	PVB-Interlayer shear modulus
G_r	Grashof number
h	Convection heat transfer coefficient (film coefficient)
h_b	Ambient side convection heat transfer coefficient
h_f	Fire side convection heat transfer coefficient
H	Glass height
k	Thermal conductivity of air
l	Flame height and can be taken equal to the window height
L	Thickness of the glass assembly
L_c	Characteristic length
P_r	Prandtl number
t_{min}	Time at which the ratio T_{gb} / T_g reaches minimum value
T_e	Temperature of the glass part covered by the frame

T_g	Temperature of the exposed glass surface
T_{gb}	Temperature of the glass' exposed surface at the ambient side
T_{gf}	Temperature of the glass' exposed surface at the fire side
T_f	Film temperature
T_i	Ambient temperature
T_∞	Temperature of the air (fire)
W	Glass width
α	Thermal diffusivity of the air
α_g	Glass' thermal expansion coefficient
α_{PVB}	PVB-Interlayer coefficient of thermal expansion
β	Thermal expansion coefficient of the air
ε	Glass' emissivity
ε_i	Middle strain
ε_s	Self-induced strain
ε_{sc}	Self-induced internal compressive strain
ε_{st}	Self-induced internal tensile strain
$\varepsilon_{t,PVB}$	PVB-Interlayer elongation at failure
ε_{th}	Unrestrained thermal strain distribution
$\overline{\varepsilon_{th}}$	Equivalent linear strain
ε_{th-eb}	Unrestrained thermal strains at the bottom covered region

ε_{th-et}	Unrestrained thermal strains at the top covered region
ε_{th-gb}	Unrestrained thermal strains at the bottom of the exposed region
ε_{th-gt}	Unrestrained thermal strains at the top of the exposed region
λ	Glass' thermal conductivity
λ_{PVB}	PVB-Interlayer thermal conductivity
ν	Glass' Poisson's ratio
ν_a	Kinematic viscosity of the air
ν_{PVB}	PVB-Interlayer Poisson's ratio
ρ	Glass' density
ρ_{PVB}	PVB-Interlayer density
σ	Stefan–Boltzmann constant
ψ_i	Curvature

Chapter 1

1 Introduction

Fire is a tragic event that can occur at any time and almost in any building. In their latest report, the Canadian Centre for Justice Statistics reported that more than 200,000 structural fires occurred between 2005 and 2014 in Canada [1]. Research on the subject of fire safety of buildings has been mostly restricted to ensure the safety of the structural elements [2–4]. Consequently, the interaction between non-structural elements, e.g., façade and glazing elements, and the fire might have been overlooked. Tragic incidents in recent years (Table 1-1) highlighted the contribution of these elements to fire severity, emphasizing the crucial need for a better understanding of their behavior in such events [5].

Table 1-1: List of fire events highlighting façade role

Building	Location	Year	Human Losses
Grenfell Tower	London, UK	2017	79 Dead & 70 Injured
The Address Downtown	Dubai, UAE	2016	16 Injured
Mariana torch	Dubai, UAE	2015&2017	-
Tamweel Tower	Dubai, UAE	2012	-
Saif Belhasa Building	Dubai, UAE	2012	2 Injured
16-storey building	Baku, Azerbaijan	2015	17 Dead & 60 Injured
Lacrosse Building	Melbourne, Australia	2014	-
18-storey building	Roubaix, France	2012	1 Dead & 1 Injured
28-storey building	Shanghai, China	2010	53 Dead & 90 Injured
Monte Carlo Hotel	Las Vegas, USA	2008	13 Injured
Marco Polo Apartments	Honolulu, USA	2017	3 Dead &12 Injured

Continuous improvements in glass manufacturing and treatment techniques such as tempering and lamination enabled usage in locations other than the traditional ones, e.g., windows and doors. Nowadays, glass can have multiple applications in buildings. These applications can be functional (glass guards, Fig. 1-1a), structural (floors, Fig. 1-1b), architectural (natural source of lighting, Fig. 1-1c), or any combination of these roles. A wide range of glass products exists in the market, each having certain behavior that suits a specific application. The growing interest in using glass in the construction industry created an additional challenge for fire safety design requirements.

Glass is a very brittle material and can quickly fail during a fire creating a new vent that increases the oxygen supply and allows smoke and flames from the fire to spread [6,7]. Much of the current literature in the field of fire safety of glass relies on experiments as part of their studies. One major drawback of such approach is that these experiments can be expensive, time-consuming, and are sensitive to the surrounding environmental conditions. Limited available studies have proposed practical methods to assess the behavior of glass during fire exposure without the need for experiments or sophisticated Finite Element (FE) modeling. This thesis aims at filling this research gap by providing a simple method to predict the behavior of glass during fire exposure.

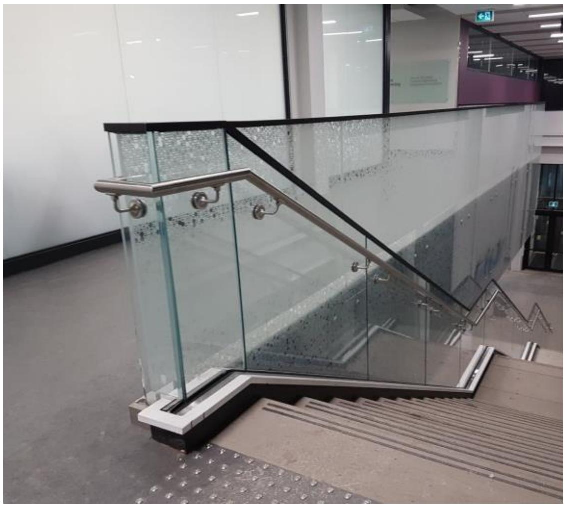

(a) Glass guards

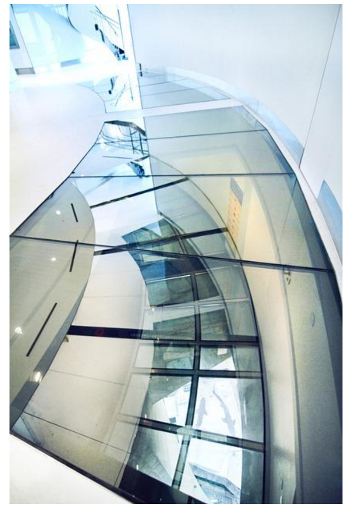

(b) Glass floor
at CN Tower, Canada

(c) Glass façade of Amit Chakma Engineering Building at Western University

Figure 1-1: Examples for different glass applications

1.1 Research Objectives

With the recent shift in the construction industry toward sustainable development, the use of glass has considerably increased in modern buildings, creating a need for a simple and reliable method to assess the behavior of glass during fire exposure. To this purpose, this research aims at:

1- Presenting a comprehensive literature review that summarizes the properties of glass panels, glass products, and structural performance at ambient temperatures and during fire exposure.

2- Developing a simple method to determine the temperature distribution in ordinary and laminated glass panels during fire exposure.

3- Developing a simple method to determine the maximum developed thermal stress in ordinary and laminated glass panels during fire exposure.

1.2 Original Contributions

This work contributes to existing knowledge of fire safety performance-based design by providing a quantitative framework for studying the behavior of ordinary and laminated glass panels during fire exposure. Simple methods were developed to allow engineers to estimate maximum thermal stresses, which are developed in glass panels during exposure to a fire.

1.3 Outline of Thesis

This thesis has been prepared in an "Integrated-Article" format. There are five chapters in this thesis. The five chapters cover the needed background information on the subject, the proposed methods, the main findings, and future recommendations.

Chapter 3

Ordinary glass is one of the most widely used materials in the construction industry. Knowing its fire resistance is essential to ensure the safety of emergency personnel as its failure increases the oxygen supply and causes a rapid spread of the fire (flashover phenomenon). Existing approaches for evaluating the structural fire safety of glass façades require expensive experimental tests and/or extensive knowledge of Finite Element modeling. This chapter provides a simplified, rational, and reliable approach to assess the structural capacity of ordinary glass panels during fire exposure. A simplified method is developed to predict the temperature difference between the edge and the center of the glass panel. Afterwards, a method, based on strain-equilibrium, is developed to predict the corresponding maximum thermal stress. The developed methods are validated by comparisons with experimental work retrieved from the open literature.

Chapter 4

With the recent shift toward sustainable development in the construction industry, the demand for using glass in modern buildings has considerably increased. One of the challenges for such a shift is its effect on the building fire safety. Glass can quickly break during fire, leading to the increase of the fire severity. This undesirable effect has been addressed by specialized codes, which require glass to maintain adequate post-breakage integrity level to protect occupants from the spread of flames and smoke. Laminated glass superior to ordinary glass in its impact resistance and sound insulation. This chapter aims at providing a simplified method to study the effect of temperature gradients on the resistance of laminated glass panels. The results of the proposed methods are validated by comparisons with experimental work by others.

Chapter 5

Chapter 5 summarizes the research outcomes and conclusions, along with providing recommendations for future research.

1.4 References

[1] Canadian Centre for Justice Statistics, Fire statistics in Canada, Selected Observations from the National Fire Information Database 2005 to 2014, 2017. Retrieved August 3, 2020, from http://nfidcanada.ca/wp-content/uploads/2017/09/Fire-statistics-in-Canada-2005-to-2014.pdf.

[2] R.T. Kuehnen, M.A. Youssef, Performance-Based Design of RC Columns using an Equivalent Standard Fire, Fire Safety Journal. 111 (2020) 102935. doi:10.1016/j.firesaf.2019.102935.

[3] R.T. Kuehnen, M.A. Youssef, Equivalent Standard Fire Duration to Evaluate Internal Temperatures in Natural Fire Exposed RC Beams, Fire Safety Journal 108 (2019) 102831. doi:10.1016/j.firesaf.2019.102831.

[4] S.F. El-Fitiany, M.A. Youssef, Fire performance of reinforced concrete frames using sectional analysis, Engineering Structures. 142 (2017) 165–181. doi:10.1016/j.engstruct.2017.03.065.

[5] K. Nguyen, P. Weerasinghe, P. Mendis, T. Ngo, J. Barnett, Performance of modern building facades in fire: a comprehensive review, Electronic Journal of Structural Engineering 16 (2016) 69–86.

[6] O. Keski-rahkonen, Breaking of Window Glass Close, Fire Technology. 12 (1988) 61–69.

[7] P.J. Pagni, A.A. Joshi, Glass Breaking In Fires, Fire Safety Science. 3 (1991) 791–802. doi:10.3801/IAFSS.FSS.3-791.

Chapter 2

2 Literature Review

Buildings need to be designed to ensure the safety of their occupants. This implies that a certain level of fire safety must be provided to minimize the risk of flame and smoke spreading. Although design of buildings emphasizes on the occupant safety, the structural engineers focus on ensuring the safety of the structural elements. Consequently, the interaction between the non-structural elements, such as façade and glazing elements, and the fire might be overlooked. This chapter covers the needed background information about the two main components of this thesis, the fire and glass.

2.1 Compartment Fires

The development of compartment fires involves the following stages: incipient, growth (pre-flashover), burning (post-flashover), and decay. Fig. 2-1 represents the time-temperature curve of a compartment fire, assuming that the fire is allowed to grow without suppression. Table 2-1 summarizes details about the characteristic of the different fire stages [1]. Incipient stage starts with the heating of the potential fuel source. Smoke detectors might detect this stage and allow occupants to prevent ignition or to evacuate early. After the ignition of the fuel, combustion would be restricted to small areas until the flashover point. At this stage, fire growth is controlled by the amount of fuel available. Post-flashover fires are ventilation controlled. Meaning that their behavior is dictated by the amount of oxygen supplied to the fire. High temperatures are reached at this stage, and the entire compartment becomes involved in the fire.

An understanding of pre-flashover fires is essential when designing for life safety, as pre-flashover fires can be easily extinguished by firefighters or by the sprinklers system [1] Hence, if flashover was delayed, for example, by limiting the fire's oxygen supply, adequate time would be available for occupants to evacuate, and for firefighters to extinguish the fire before it shifts to the post-flashover stage. The oxygen supply of the fire is directly related to the openings in the building envelope. Broken windows or opened ones can rapidly increase the fire burning rate, and cause flashover to immediately occur.

Table 2-1: Characteristic of fire stages [8].

Fire Stage	Incipient	Growth	Burning	Decay
Fire Behaviour	Heating of fuel	Fuel controlled burning	Ventilation controlled burning	Fuel controlled burning
Human Behaviour	Prevent ignition	Extinguish by hand, escape	Death	
Detection	Smoke detectors	Smoke detectors, heat detectors	External smoke and flame	
Active Control	Prevent ignition	Extinguish by sprinklers or fire fighters; control smoke	Control by fire fighters	
Passive Control	-	Select materials with resistance to flame spread	Provide fire resistance; contain fire, prevent collapse	

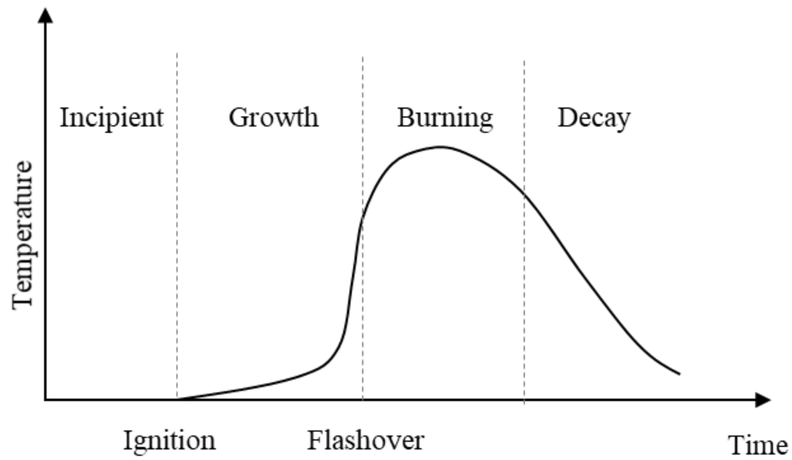

Figure 2-1: Compartment fire curve

2.2 Glass in Buildings

For aesthetic, lighting, and energy requirements, the use of glass has considerably increased in buildings' envelope. Building codes mandate the use of fire-rated glass or safety glass such as wired or laminated glass in certain locations to limit the spreading of flames and smoke. This section provides the needed background on the material properties, production method, and types of glass products.

2.2.1 Chemical Composition

Glass is an inorganic and non-crystalline solid. Its behavior is challenging to study because of its non-crystallinity. For example, glass does not have a fixed melting point. Rather, at elevated temperatures, glass gradually changes its state from solid to viscoelastic and finally to a liquid state. The temperature at which molten glass becomes solid is called the transformation temperature and it is around 530 ºC for Soda-lime glass [2].

Soda-Lime-Silica glass (soda-lime glass) is the most available type in the market. It is composed of Silicon dioxide (silica), SiO_2. Pure silica itself has excellent resistance to thermal shock and has a high melting temperature (1723 ºC) [3]. However, because of its high viscosity, it has low workability during manufacturing. Other oxides are added such as Sodium oxide Na_2O to decrease its viscosity and melting temperature. These additives also slightly increase the elasticity of the glass. Calcium oxide, CaO, is added to improve the chemical resistance of the glass. Aluminum oxide, Al_2O_3, potassium oxide, K_2O, iron (III) oxide (ferric oxide), Fe_2O_3, titanium dioxide, TiO_2, and magnesium oxide (magnesia), MgO, are also added to provide better chemical durability for the glass. Changing the percentage of any additive affects the properties of the final glass product. Typical material composition for soda-lime glass is listed in Table 2-2 [4].

Table 2-2: Typical Soda-lime glass compostion

Oxide	Range (%)
SiO_2	69 – 74
Na_2O	10 – 16
CaO	5 – 14
MgO	0 – 6
Al_2O_3	0 – 3
Others	0 – 5

2.2.2 Material Properties

Glass is homogenous, isotropic, and perfectly elastic. The elastic nature of glass does not allow for plastic deformation to occur, and, thus local stress concentrations, around holes or flows, are not reduced. This brittle behavior is a concern when considering using glass as a structural element [5]. The tensile strength of glass is not a material constant. It depends on various factors such as surface condition, initial flaws, characteristics of these flaws (size and depth), loading history (intensity and duration), residual stresses (heat or chemical strengthening), and surrounding environmental conditions (humidity). Thus, even though the theoretical tensile strength based on molecular forces of glass can reach up to 10 GPa [2], this strength is not useful for engineering purposes since glass will fail at significantly lower stress values. The failure happens when the tensile stresses approach or exceed the ultimate strength at the tip of a flaw. The compressive strength of glass is much higher than its tensile strength. Because the presence flaws has no effect on its compressive strength. The average compressive strength of glass ranges from 880 to 930 MPa [6]. Table 2-3 summarizes some of the most important properties of soda-lime glass.

Table 2-3: Soda-Lime glass properties

Parameter	Symbol	Value	Unit
Density	ρ	2500	kg/m^3
Young's modulus	E	70	GPa
Poisson's ratio	ν	0.23	dimensionless
Coefficient of thermal expansion	α_g	9	10^{-6} K^{-1}
Specific heat	c	720	Jkg^{-1} K^{-1}
Thermal conductivity	λ	1	Wm^{-1} K^{-1}
Emissivity (corrected)	ε	0.837	dimensionless

2.2.2.1 Tensile Strength at Ambient Temperature

Bansal and Doremus [7] reported that the tensile strength of glass in dry (inert atmosphere) is 70 MPa. However, at 50% relative humidity, glass will lose one-third of its inert strength. A value of 20 MPa was suggested for the effective strength of the glass. Pagni and Joshi [8] performed 59 experiments using the four-point flexural test on ordinary float glass. The data from experiments were fitted into a three-parameter cumulative Weibull function to determine the glass breaking stress and a breaking stress of 40 MPa was recommended. Pagni [9] suggested that the breaking stress for soda lime float glass ranges from 10 to 50 MPa at a temperature of 50°C considering different edge conditions and stress histories.

Vandebroek et al. [10] performed four-point bending test on ordinary glass samples with different edge conditions (polished and cut edges). The samples were tested at a high loading rate (55 MPa/s ± 10 MPa/s) and a low loading rate (0.55 MPa/s ± 0.10 MPa/s). The reported tensile strengths corresponding to a linearly increasing load (nom) and a constant load (equiv) are summarized in Fig. 2-2 below [10,11].

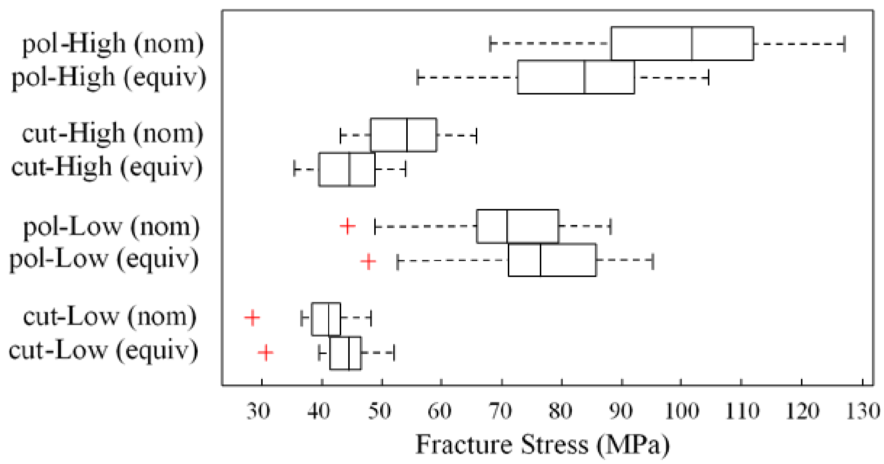

Figure 2-2: Boxplots of glass fracture stress

2.2.2.2 Tensile Strength at Elevated Temperatures

Xie et al. [12] conducted direct tensile testing on ordinary float glass. Fig. 2-3a shows the average breaking stresses for different thickness values at ambient and 200 ºC. The flocculation in the breaking stress values confirms that the presence of initial flaws has an effect on the tensile strength of glass. Wang et al. [13] performed a series of direct tensile test experiments on ordinary float glass with a thickness of 6 mm during heating. Fig. 2-3b shows the average and minimum breaking stress values at different elevated temperatures. Li et al. [14] studied the fracture behaviour of ordinary glass at elevated temperature. The bending strength of the glass samples were measured using the three-point bending. The results are summarized in Fig. 2-3c [14].

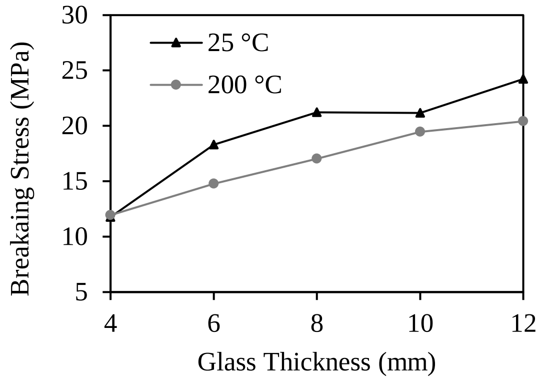

(a) Experiments by Xie et al. [12]

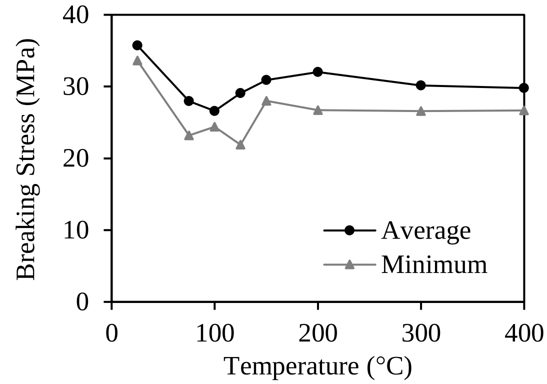

(b) Experiments by Wang et al. [13]

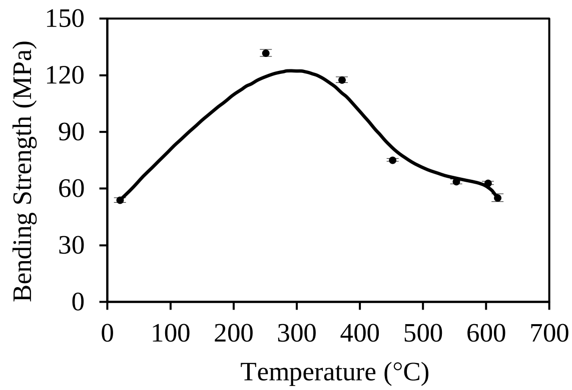

(c) Experiments by Li et al. [14]

Figure 2-3: Glass breaking stress at elevated temperature

2.2.3 Glass Production

Most of the modern glass is known as float glass. It is produced as large-size panels using the floating process, which was introduced in 1959 by Sir Alastair Pilkington [15]. In this production process, a continuous ribbon of glass is formed by pouring molten glass (1000 ºC) on top of molten tin and left until all the irregularities melt and the molten glass spreads to form a flat surface. The glass ribbon is then cooled until it becomes hardened enough (600 ºC) to be removed from the top of the tin. It is then transferred into a temperature-controlled kiln (Annealing Lehr), where it is slowly cooled to minimize the residual stresses. The outcome of this process is a ribbon of annealed float glass, which then can be cut to the desired sizes. Fig. 2-4 shows a schematic diagram of the floating process [16]. Float glass paved the way for the development of other types of glass with improved properties, which will be summarized in the following section.

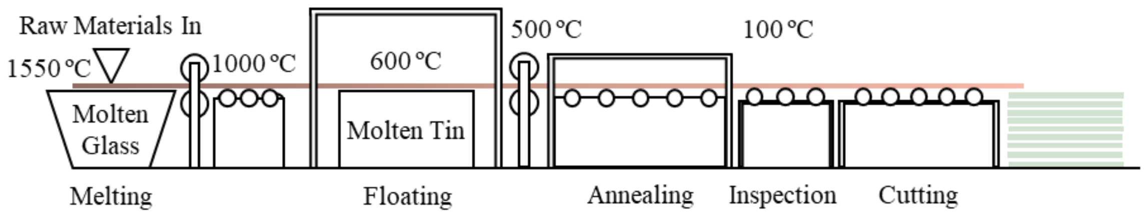

Figure 2-4: Float glass production process

2.2.4 Glass Products

2.2.4.1 Float Glass (Annealed Glass/ Flat Glass)

Float glass is the most basic, least expensive, and most commonly available glass product in the market. Its resistance to fire and external loads is limited. However, it is the base product to produce glass panels with improved properties. When it breaks, large fragments of glass fallout (Fig. 2-5a).

2.2.4.2 Toughened Glass (Fully tempered glass)

Toughened glass is approximately three times stronger than ordinary float glass [17]. It is strengthened by the tempering process where float glass is heated and then cooled rapidly. During the tempering process, surfaces of the glass will cool faster than the inner core creating high compressive stresses at the glass surfaces and tensile stresses at the inner core (Fig. 2-6). This state of stress causes the glass to shatter into granular pieces when broken (Fig. 2-5b). This failure pattern is desired to reduce injuries where human impact is expected such as in glass tables, doors, and glass dividers. However, it is undesired for fire safety applications since it does not provide any post-breakage integrity.

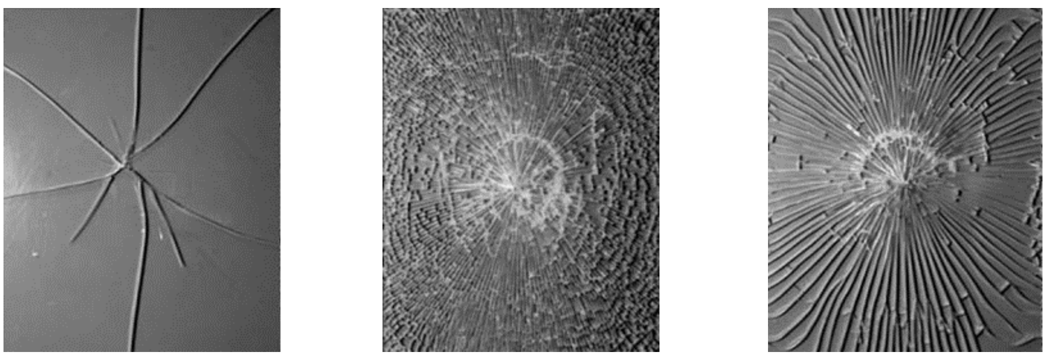

(a) annealed glass (b) Toughened glass (c) heat strengthened glass

Figure 2-5: Fracture pattern for different types of glass

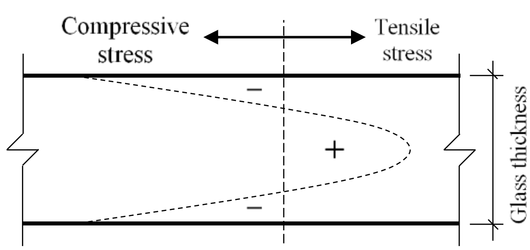

Figure 2-6: Residual stress profile due to tempering process

2.2.4.3 Heat-Strengthened Glass

This type of glass is approximately twice as strong as annealed glass [17]. It is similar to the toughened glass since both require heating the float glass to high temperatures and then cooling it. However, the cooling process for the heat-strengthened glass is slower than that for the toughened glass. Thus, the stresses generated within the glass during the process are lower than that for the toughened glass. When it breaks, the heat-strengthened glass panel breaks into large pieces that usually remain at its location (Fig. 2-5c) [5].

2.2.4.4 Laminated Glass

Laminated glass is manufactured by permanently bonding two or more glass panels separated by interlayers. When laminated glass cracks, the broken pieces usually do not fall out; rather, they adhere to the interlayers through shear interaction [18]. Because of this post-cracking behavior, laminated glass is a great choice for safety purposes, as it reduces injuries from falling glass. In addition, it prevents the creation of new openings during a fire. The most common interlayer material is Polyvinyl Butyral (PVB); however, other materials can be used such as Ethylene-Vinyl Acetate (EVA) or SentryGlas® (SG). The nominal thickness of a single PVB layer is 0.38 mm. PVB is a viscoelastic material and its physical properties are highly dependent on the temperature and the load duration. PVB is relatively soft and ductile at room temperature and it has a breakage elongation of more than 200%. Haldimann et al. [5] suggested that at temperatures well below 0ºC and for short duration loads, PVB is able to transfer the full shear stress from one panel of glass to another. On the other hand, for higher temperatures and long duration loads, the shear transfer is greatly reduced. Table 2-4 lists typical properties of PVB interlayer [5].

The glass panels that are used in the laminating process can be ordinary float glass, Heat-strengthened glass, toughened glass, or a combination of those types. Depending on the type used for the laminating process, the post-breakage behavior of the assembly will change (Fig. 2-7). For example, laminated glass composed of toughened glass panels is susceptible to shatter into highly fragmented pieces and therefore, it will not provide any post-breakage stability by means of arching or locking action and the stability will be only limited by the tensile strength of the interlayer. The tensile strength of the PVB interlayer tends to tear causing large deformations that can lead to the glass sliding out from its supports and eventually collapsing. Using a combination of ordinary float glass or heat strengthened glass panels with fully tempered panels will improve the behavior of the assembly and increase the stability as long as the fully tempered glass panels are located on the tension side of the laminated unit [5]. Behr et al. [19] indicated that at the room temperatures, laminated glass with polyvinyl butyral (PVB) interlayers has similar behavior as ordinary float glass of the same nominal thickness under short-term lateral loading (e.g. wind loads). It was also suggested that the temperature at which the behavior changes is around 49°C. For long-term lateral loading (e.g. snow loads), the behavior of laminated glass will be similar to ordinary float glass at temperatures of 0°C and below [19].

Table 2-4: PVB interlayer properties

Parameter	Symbol	Value	Unit
Density	ρ_{PVB}	1070	kg/m^3
Shear modulus	G_{PVB}	0 – 4	GPa
Poisson's ratio	ν_{PVB}	≈0.50	Dimensionless
Coefficient of thermal expansion	α_{PVB}	8	10^{-6} K^{-1}
Tensile strength	$f_{t,PVB}$	≥20	MPa
Elongation at failure	$\varepsilon_{t,PVB}$	≥300	%

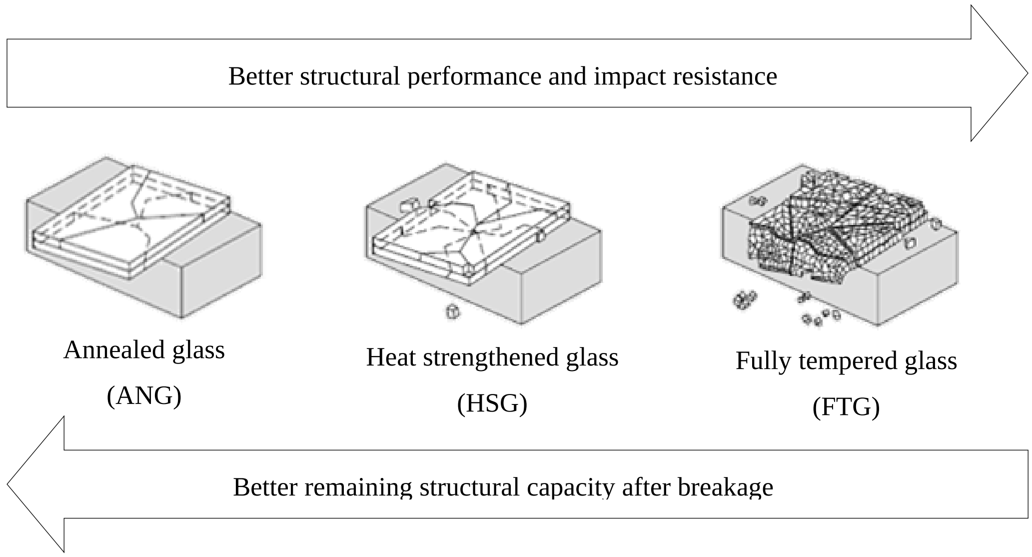

Figure 2-7: Post breakage behavior of laminated glass

Norville et al. [20] used engineering mechanics to present a theoretical model to study the behavior of laminated glass under the effect of different heating rates, different interlayer material thicknesses, and different interlayer material types. It was indicated that the strength of laminated glass increases as the interlayer thickness increases and decreases as the temperature increases [20].

The flexural behavior of laminated glass can be classified into three stages. To demonstrate these stages, Fig. 2-6 has an example of a laminated glass assembly that consist of two ordinary glass panels with PVB-interlayer undergoing an increase in loading. The first stage, when the tensile stresses are low, both glass panels remain intact. When the stresses increase in the second stage, the bottom glass panel fractures and only the top panel will carry the loads. Finally, when the tensile stress reaches the breaking stress, the top glass panel will also fracture, however, the interlock action between the fragments in the top panel in the compression zone combined with the slight contribution from the tensile stress in the interlayer provides some post-breakage resistance.

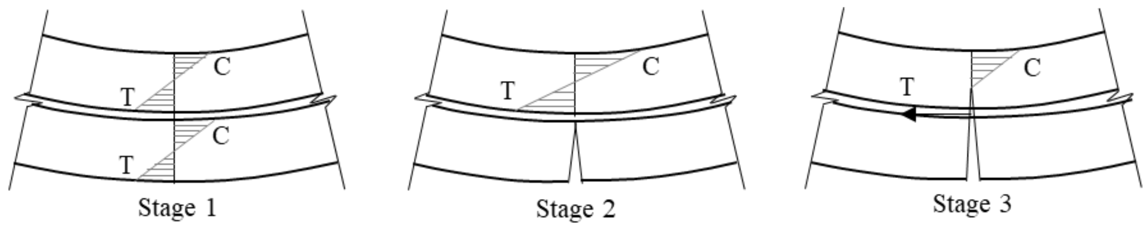

Figure 2-8: Stages of flexural bending in laminated glass

2.2.4.5 Tinted Glass

This type of glass is made by adding coloring materials to the raw materials while manufacturing the glass. Tinted glass has higher heat absorption than ordinary clear glass, since the coloring materials reduce the transmittance of the glass. This additional heat could cause extra thermal stresses in the glass which may affect the behavior of the glass and make it more prone for breakage [21].

2.2.4.6 Wired Glass

Wired glass is a type of glass that has a welded wire net integrated with the glass. Wired glass is considered as a safety glass because of the wire ability to hold the glass in it is place in case of a breakage. This prevents new vents from forming and reduces the risk of injuries by falling glass. However, the addition of the wires increases the flaws in the glass. Hence, wired glass usually has lower strength than ordinary glass [22].

2.3 Thermal Breakage of Glass

Emmons [23] first suggested that the glass breakage mechanism in fire is thermally-induced tensile failure caused by the differential heating between the glass center and the part covered by the frame. Internal thermal stresses develop because of this differential heating and cracks occur when the internal stresses exceed the glass strength. These cracks can propagate and expand quickly through the panel, leading to the fallout of glass [24]. This phenomenon, in which failure occurs due to differential expansion caused by thermal gradient, is referred to as thermal shock.

Glass resistant to thermal shock was initially defined in terms of an allowable temperature gradient within the glass panel. Researchers reported different temperature gradients considering type of glass, heating intensity, glass panel size, and boundary conditions [25]. In addition, in all the studies, the breaking stress of the glass was unkown and reserachers had to conudct experiemntal tests or to make an assumption to determine the tensile strength of the glass.

Keski-Rahkonen [26] did an extensive theoretical analysis that addressed the cracking behavior of glass during fire exposure. Analytical equations for quasi-static thermal stress field in the glass panel were derived based on thermal fields that are calculated from the conduction equation with linearized radiation cooling boundary conditions. Using ordinary float glass (E = 80 GPa, α_g = 8 × 10^{-6} C^{-1}, and taking the maximum tensile stress from tensile tests as σ_y = 50 MPa), the relationship between tensile stress in the glass at failure (σ_y) and the temperature difference between the heated portion and the protected edge of the glass (ΔT) was simplified as given by Eq. 2-1. Thus, the approximate maximum temperature difference at breaking was suggested to be equal to 80 ºC.

$$\sigma_y = \alpha_g \, E \Delta T \tag{2-1}$$

Pagni [27] predicted that glass first cracks at a temperature difference of 58 ºC. This difference in results among researchers is due to the variabilities in glass properties. Pagni also referenced a fracture mechanics computer simulation done at Berkeley that obtained a temperature difference at failure equal to 60º C.

Skelly et al. [28] conducted an experimental investigation using ordinary float glass (E = 70 GPa, σ_y = 47 MPa, and α_g = 9.5 × 10^{-6} C^{-1}) to examine the role of the unheated edge on glass breaking behavior during fire. Glass with unprotected edges were found to break at 197 ºC, while for edge protected glass, breakage happened at 90º C. This experiment resulted in 30% higher than the temperature predicted by the theoretical study of Keski-Rahkonen, which was 70º C. The difference was attributed to the radiative heating of the thermocouple on the center of the glass.

Pagni and Joshi [24] quantified the glass central temperature profile history for any fire exposure, which lead to the evaluation of the mean stress history. Then, the problem was simplified by assuming the temperature gradients along the planer directions to be equal to zero. Furthermore, the temperature at the edges was assumed to remain at the ambient temperature, provided that the covered part is large, and the heating rate is fast. The central temperature history was written in terms of change in temperature across the glass thickness with time. It was suggested that regardless of the glass panel size, the breakage stress of float glass is approximately 40 MPa.

Harada et al. [22] conducted 50 experiments on float and wired glass and developed a simple model to predict the glass cracking stress under radiant heating. The measured parameters in their experiments were, the time for initial crack, the temperature at the center of glass pane, and the edge strain and temperature. It was found that the ultimate stress for float glass ranges from 15 to 35 MPa and from 3 to 13 MPa for wired glass.

Wang et al. [29] studied the effect of changing the glass panel dimensions on the structural resistance of glass during fire exposure. The testing was done on two glass panels with dimensions of 300 mm by 300 mm by 6 mm and 600 mm by 600 mm by 6 mm. Then, numerical models were created for glass panel with dimensions ranging from 100 mm by 100 mm to 1000 mm by 1000 mm with aspect ratios of 400:1, 100:1, 25:1, 25:4, 4:1 and 25:16. The thickness of glass panels was kept constant between the runs at 6 mm. It was established that smaller size glass panels and glass panels with larger aspect ratio had better fire resistance.

Dembele et al. [30] presented a study that investigates the effect of boundary conditions on the thermal breakage of ordinary float glass in compartment fires. The study shows that providing adequate space between the protected-edge glass panel and the frame minimizes the risk of glass failure and delays cracking. In addition, three edge conditions were investigated: as-cut edge, ground edge, and polished edge. For the specific test conditions, it was established that the “as-cut” edge finishing is stronger and has longer failing time compared to the ground and polished edges finishing.

Chow et al. [31] investigated the relative significance of the two temperature gradient components (across the thickness and in planar direction) on the glass breakage, and assessed the contributions of these components on the total thermal stress. They concluded that the temperature gradient component across the thickness is much larger than that in the planar directions and the heat boundary condition of the backside has a significant influence on the temperature gradient component across the thickness and little influence on the temperature gradient components in the planar direction. However, it was suggested that the temperature gradient component across thickness can be ignored as it is unlikely to cause breaking. Furthermore,

Harada et al. [22] analyzed the post-cracking behavior of wired glass and ordinary float glass. It was found out that the post-cracking behavior depends mainly on the imposed heat flux and slightly on the restrains of the glass. Under extreme heating (more than 9 kW/m^2) the glass will fall out in large pieces.

2.4 Summary

This chapter presented an overview of the fire behavior at different stages, glass properties, glass products, and the available literature on the thermal breakage of the glass. Several important factors, which affect the behavior of glass, were highlighted. The important points, which were presented in this chapter, are summarized below.

1. The tensile strength of the glass is a complex quantity. The discrepancy between the results of the reported experimental tests on glass samples does not allow defining the tensile strength of glass at elevated temperatures.
2. Several glass products are available in the market. Specialized codes require glass to maintain a certain level of post-breakage integrity to prevent flames and smoke

spreading during fire. Heat-treated glass has higher structural capacity as compared to ordinary glass. However, it is not necessarily favored for fire safety as it shatters when it breaks. Wired glass used to be the favored choice, as the wires hold broken glass pieces together. This belief was changed, when it was proven that the wires reduce the impact resistance of the glass and can cause injuries upon impact.

3. As most studies rely on experimental work to study the behavior of glass during fire exposure, there is a clear lack of simplified methods to determine the stresses developed during fire exposure.

2.5 References

[1] A.H. Buchanan, A.K. Abu, Structural design for fire safety, John Wiley & Sons, 2017.

[2] M. Haldimann, A. Luible, M. Overend, Structural use of Glass, 2006.

[3] J.J. Lagowski, Chemistry: Foundations and Applications, ISBN 0-02-865724-1, 2004.

[4] S.M. Karazi, I.U. Ahad, K.Y. Benyounis, Laser Micromachining for Transparent Materials, (2017).

[5] M. Haldimann, A. Luible, M. Overend, Structural use of glass, International Association for Bridge and Structural Engineering, Zürich, Switzerland, 2008.

[6] M. Fröling, Strength design methods for laminated glass, (n.d.).

[7] N.P. Bansal, R.H. Doremus, Handbook of glass properties. 1986, (n.d.).

[8] A.A. Joshi, P.J. Pagni, Fire-induced thermal fields in window glass. II—Experiments, Fire Safety Journal. 22 (1994) 45–65. doi:10.1016/0379-7112(94)90051-5.

[9] P.J. Pagni, Thermal glass breakage, Fire Safety Science. (2003) 3–22. doi:10.3801/IAFSS.FSS.7-3.

[10] M. Vandebroek, J. Belis, C. Louter, G. Van Tendeloo, Experimental validation of edge strength model for glass with polished and cut edge finishing, Engineering Fracture Mechanics 96 (2012) 480–489. doi:10.1016/j.engfracmech.2012.08.019.

[11] D. Kinsella, Modelling of Annealed Glass Fracture, Lund University, 2018.

[12] Q. Xie, H. Zhang, D. Si, Experimental study on critical breakage stress of float glass with different thicknesses under conditions with temperatures of 25 and 200 C, Fire Mater. 35 (2011) 275–283.

[13] Y. Wang, Q. Wang, G. Shao, H. Chen, J. Sun, L. He, K.M. Liew, Experimental study on critical breaking stress of float glass under elevated temperature, Mater. Des. 60 (2014) 41–49. doi:10.1016/j.matdes.2014.03.038.

[14] D. Li, W. Li, R. Wang, X. Shen, Temperature dependence of the three-point bending fracture behavior of soda-lime-silica glass with surface scratch, J. Non. Cryst. Solids. 409 (2015) 126–130. doi:10.1016/j.jnoncrysol.2014.11.025.

[15] L.A.B. Pilkington, Review lecture: the float glass process, Proc. R. Soc. London. A. Math. Phys. Sci. 314 (1969) 1–25.

[16] M. Patterson, Structural glass facades and enclosures, John Wiley & Sons, 2011.

[17] M. Kozlowski, C. Bedon, D. Honfi, Numerical analysis and 1D/2D sensitivity study for monolithic and laminated structural glass elements under thermal exposure, Materials (Basel). 11 (2018). doi:10.3390/ma11081447.

[18] M. Debuyser, J. Sjöström, D. Lange, D. Honfi, D. Sonck, J. Belis, Behaviour of monolithic and laminated glass exposed to radiant heating, Construction and Building Materials 130 (2017) 212–229. doi:10.1016/j.conbuildmat.2016.09.139.

[19] R.A. Behr, J.E. Minor, H.S. Norville, Structural behavior of architectural laminated glass, Journal of Structural Engineering. 119 (1993) 202–222.

[20] H.S. Norville, K.W. King, J.L. Swofford, Behavior and strength of laminated glass, J. Eng. Mech. 124 (1998) 46–53.

[21] A. Vedrtnam, C. Bedon, M.A. Youssef, M. Wamiq, A. Sabsabi, S. Chaturvedi, Experimental and numerical structural assessment of transparent and tinted glass during fire exposure, Construction and Building Materials. 250 (2020). doi:10.1016/j.conbuildmat.2020.118918.

[22] K. Harada, A. Enomoto, K. Uede, T. Wakamatsu, An experimental study on glass cracking and fallout by radiant heat exposure, Fire Safety Science. (2000) 1063–1074. doi:10.3801/IAFSS.FSS.6-1063.

[23] H.W. Emmons, The needed fire science, in: Fire Safety Science First International Symposium, IAFSS, 1986: pp. 33–53.

[24] P.J. Pagni, A.A. Joshi, Glass Breaking In Fires, Fire Safety Science 3 (1991) 791–802. doi:10.3801/IAFSS.FSS.3-791.

[25] C. Bedon, M. Kozłowski, D. Honfi, Thermal assessment of glass façade panels under radiant heating: Experimental and preliminary numerical studies, J. Facade Des. Eng. 6 (2018) 049–064. doi:10.7480/jfde.2018.3.2477.

[26] O. Keski-rahkonen, Breaking of Window Glass Close, Fire Technology 12 (1988) 61–69.

[27] P. Pagni, Fire Physics - Promises, Problems, And Progress, Fire Safety Science 2 (1989) 49–66. doi:10.3801/iafss.fss.2-49.

[28] M.J. Skelly, R.J. Roby, C.L. Beyler, Experimental investigation of glass breakage in compartment fires, J. Fire Prot. Eng. 3 (1991) 25–34. doi:10.1177/104239159100300103.

[29] Y. Wang, Y. Zhang, Q. Wang, Y. Yang, J. Sun, The effect of glass panel dimension on the fire response of glass façades, Construction and Building Materials 181 (2018) 588–597. doi:10.1016/j.conbuildmat.2018.06.088.

[30] S. Dembele, R.A.F. Rosario, J.X. Wen, Thermal breakage of window glass in room fires conditions - Analysis of some important parameters, Build. Environ. 54 (2012) 61–70. doi:10.1016/j.buildenv.2012.01.009.

[31] Y. Yang, L. Miao, C.L. Chow, Relative significance of temperature gradient components on cracking behavior in glass panes under thermal radiation, Appl. Therm. Eng. 131 (2018) 837–848. doi:10.1016/j.applthermaleng.2017.12.060.

Chapter 3

3 Simplified Structural Analysis of Ordinary Glass Panels during Fire Exposure

Fire safety has been mostly restricted to structural elements [1–4]. Consequently, the interaction between the non-structural elements, e.g. glazing elements, and the fire has been overlooked [5]. Nevertheless, recent tragic incidents (e.g., Grenfell Tower fire, UK) emphasized the key role of these elements during such events [6].

During a fire event, failure of glass panels creates new vents, which increases the oxygen supply, leading to a wide spread of smoke and flames. This failure is caused by the thermal gradient between the center and edge of the heated glass panels [7–9]. These thermal gradients occur because of the isolation provided by the supporting frame and the glass low thermal conductivity.

Several experimental [10–18] and numerical studies [19–23] were conducted to predict the thermal and structural behavior of glass panels during fire events. These studies highlighted some key factors, which affect the fire resistance of glass panels, including the effect of the applied heat flux [11,24], fire location [12,13], temperature gradients [18], size of glass panels [16,22,23], edge finishing conditions [19], and installation method [17,25].

Much of the current literature about fire safety of glass relies on experiments or advanced analysis using the FE method. These approaches are expensive and/or time-consuming. To the best of the author's knowledge, the literature is lacking simplified analysis techniques that can facilitate applying performance-based design concepts, while designing building facades. This chapter addresses this research gap by providing a simple approach to predict the behavior of glass during fire exposure. The approach provides the means to predict the temperature gradient caused by the fire event and, then, predict the maximum developed thermal stress.

3.1 Temperature of Glass during Fire Exposure

In this section, a simplified approach is developed to predict the temperatures at the center and the edge of glass panels exposed to fire. As a conservative assumption, the part of the glass panel, which is covered by the supporting frame, is assumed to be unaffected by radiation and convection of the flames. Therefore, it is only heated through conduction from the exposed part of the glass. This assumption simplifies heat transfer calculations and eliminates the need for considering the heat exchange between the frame and glass (Fig. 3-1). The approach starts by deriving a heat transfer equation to determine the temperature at the center of the glass panel, and, then, uses this temperature to evaluate the temperature of the protected part.

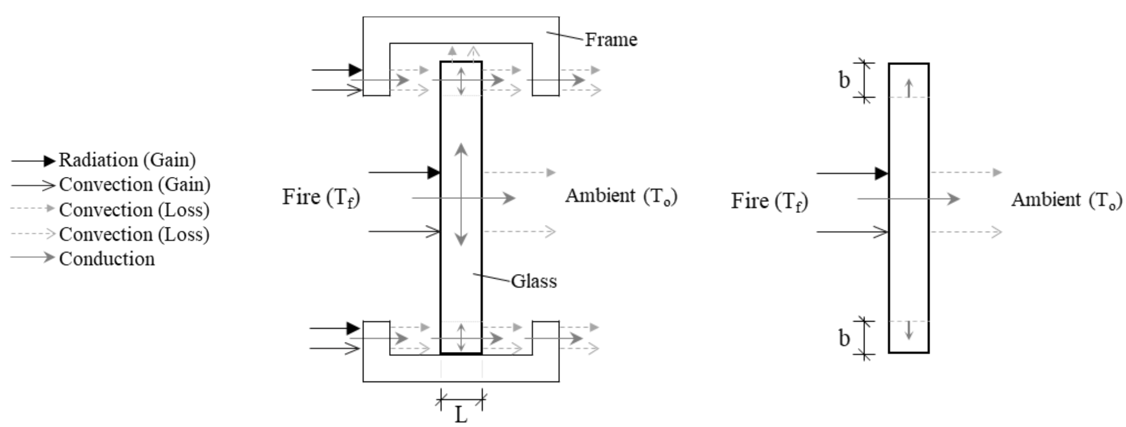

(a) Heat transfer system (b) Simplified system

Figure 3-1: Heat transfer system for glass during fire exposure

3.1.1 Temperature at the center of the glass panel

During an actual fire, temperature of the glass panel depends on many factors including the location of the fire relative to the panel, size of the panel, and air movement within the compartment. Assuming no energy generation within the glass, the transit temperature field for the case of a glass panel exposed to fire from one side, while the other side remains at ambient temperature (Fig. 1a), can be determined from the heat diffusion equation (Eq. 3-1).

$$\lambda\left(\frac{\partial}{\partial x}\left(\frac{\partial T(x,y,z,t)}{\partial x}\right)+\frac{\partial}{\partial y}\left(\frac{\partial T(x,y,z,t)}{\partial y}\right)+\frac{\partial}{\partial z}\left(\frac{\partial T(x,y,z,t)}{\partial z}\right)\right)=\rho c\frac{\partial T(x,y,z,t)}{\partial t} \quad (3\text{-}1)$$

Where, λ is the thermal conductivity of the glass, ρ is the glass density, and c is the glass specific heat. Solving Eq. 3-1 is mathematically complex and can be simplified by discretizing the system into smaller sub-systems (e.g. solving using Finite Difference Method). In this chapter, it is assumed that the uncovered glass surface is exposed to a uniform fire temperature. Furthermore, as a conservative and widely used assumption in structural fire engineering, the fire and air are assumed to be stagnant. This assumption leads to free convection between the air and the glass panel. For this case, the convection heat transfer coefficient, film coefficient (h), typically ranges from 5 to 25 W/m^{2}K [26]. For the case of vertical glass panel, the value of h can be calculated using the following empirical equations [27].

$$h = \frac{0.59 \cdot k \cdot (G_r P_r)^{\frac{1}{4}}}{l} \quad (3\text{-}2)$$

$$G_r = \frac{g \cdot l^3 \cdot \beta \cdot \left(T_\infty - T_g\right)}{{\nu_a}^2} \quad (3\text{-}3)$$

$$P_r = \frac{\nu_a}{\alpha} \tag{3-4}$$

$$\beta = \frac{1}{T_f} \tag{3-5}$$

Where, l is the flame height and can be taken equal to the window height, k is the thermal conductivity of air, G_r is Grashof number, P_r is Prandtl number, T_∞ is the temperature of the air, T_g is the temperature of the glass surface, g is the gravitational acceleration, ν_a is the kinematic viscosity of the air, α is the thermal diffusivity of the air, β is the thermal expansion coefficient of the air, and T_f is the film temperature and can be calculated as the average temperature between the air and the glass surface [28].

The air temperature is taken equal to the fire temperature at the exposed side of the glass and the ambient temperature (T_i) at the unexposed side of the glass. The temperature gradient across the glass panel thickness can be assumed uniform. This assumption is based on the fact that the Biot number ($Bi = \frac{hL_c}{\lambda}$) of typical glass panels is expected to be less than or equal 0.1, where L_c can be taken equal to the glass thickness (L). This Bi value means that the resistance to conduction within the glass is much less than the resistance to convection at the air boundary layer [27]. Given the above-mentioned assumptions, the conservation of energy at any time instant t can be expressed by Eq. 3-6. This equation can be utilized to calculate the temperature of the glass at each time step for both standard and natural fire curves using a simplified spreadsheet.

$$\Delta T = \frac{\Delta t}{\rho c L}\left[h_f\left(T_\infty - T_g\right) + \varepsilon\sigma\left({T_\infty}^4 - {T_g}^4\right) - h_b\left(T_g - T_i\right) - \varepsilon\sigma\left({T_g}^4 - {T_i}^4\right)\right] \tag{3-6}$$

Where Δt is the time increment, ε is the emissivity of the glass and can be assumed equal to 0.85 [29], and σ is the Stefan–Boltzmann constant.

3.1.2 Temperature at the edge of the glass panel

Based on the assumption that the edge of the glass panel is only heated via conduction from the exposed parts, a parametric study was conducted using the commercial software Abaqus [30] to determine the ratio between the temperature of the protected part (T_e) and the temperature of the exposed part (T_g). Heating of the exposed part of the glass, Fig. 3-2a, was simulated as uniform surface interaction that involved radiation and convection. For such a case, the change in the glass dimensions will not affect the ratio between T_e and T_g. The only parameters that need to be considered are the glass thickness (L), width of the frame (b), and the fire scenario. The glass thickness and width of supporting frame were assumed to range from 1 mm to 15 mm and 5 mm to 50 mm, respectively. These ranges deemed to cover most of the practical values available in the literature. Assuming ISO 834 temperature-time relationship [31], 148 cases were analyzed. It should be noted that the analysis cases also represent the heating region of natural fire curves.

The material properties were assumed as follows ρ = 2500 kg/m^3 and c = 820 J/kg·K. The ambient temperature was set to 20°C. The glass panel was modeled using 8-node-3D linear-heat transfer brick elements (DC3D8 type from Abaqus library). A maximum mesh size of 10 mm was utilized, as it was found to result in acceptable accuracy. An example of the generated mesh is shown in Fig. 3-2b. The temperature of point A (Fig. 3-2a) was recorded for each run, and this temperature was assumed to represent the temperature of the covered part. A typical temperature distribution, as produced by ABAQUS, is shown in Fig. 3-3. Also, the typical variation of the ratio $\frac{T_e}{T_g}$ with time is shown in Fig. 3-4.

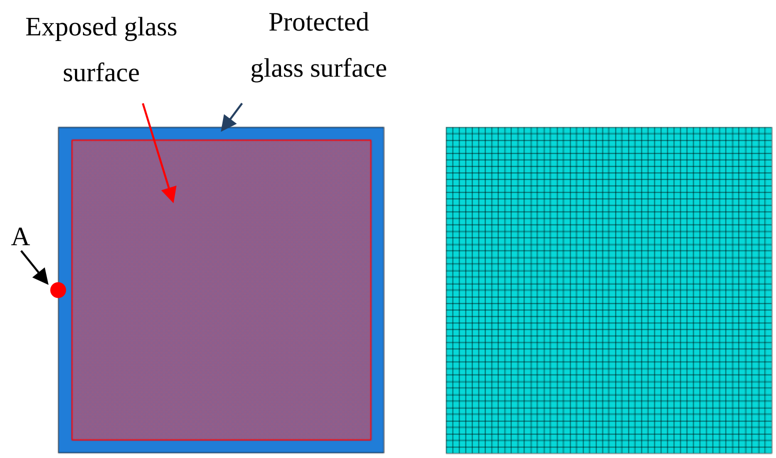

(a) glass panel zones (b) generated mesh

Figure 3-2: Glass Panel Simulation using ABAQUS

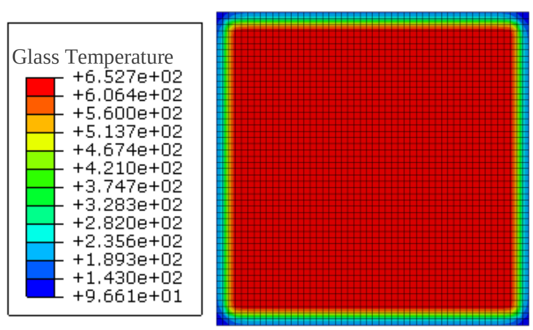

Figure 3-3: ABAQUS Temperature Distribution (L = 6 mm, b = 20 mm, t = 30 minutes)

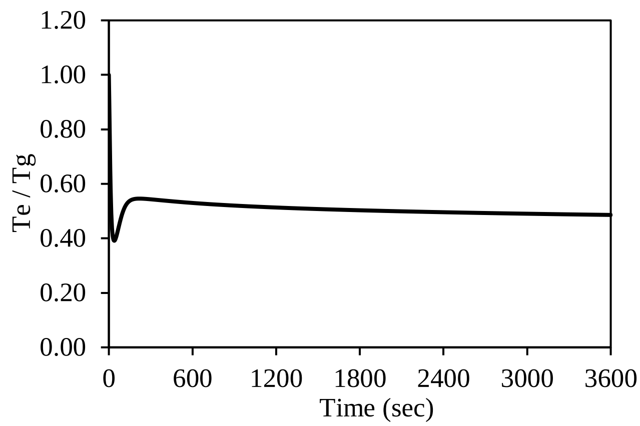

Figure 3-4: Variation of T_e / T_g with time (L = 1 mm and b = 5 mm)

Initially, the exposed and protected parts of the glass had the same temperature, and, then the ratio between their temperatures started to change until reaching a constant value. Considering all examined cases, the average $\frac{T_e}{T_g}$, for the relatively constant part of the variation, is given in Fig. 3-5 as function of the frame width and glass thickness. The temperature difference between the center and edge of the glass panel increases with increasing the glass thickness and decreases with increasing the frame width. Engineers can utilize this figure to calculate this ratio. To further simplify calculation of $\frac{T_e}{T_g}$, the figure data were utilized to develop the formula given by Eq. 3-7, which allow calculating $\frac{T_e}{T_g}$ as function of *b* (m) and *L* (m). The equation and coefficients were determined using a least square regression analysis, common regression requirements of probability (p) < 0.0001 and correlation (R^2_{adj}) > 95% were maintained. The maximum error associated with using Eq. 3-7 is less than 6%, as shown in Fig. 3-6.

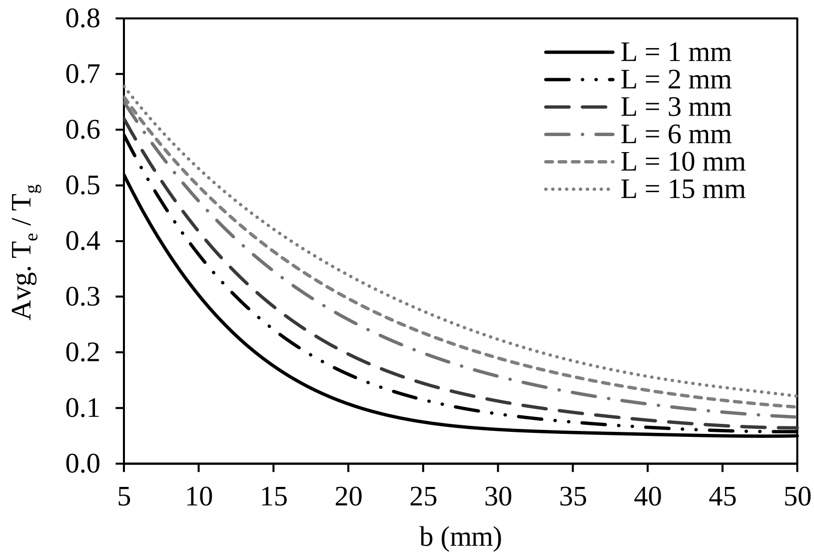

Figure 3-5: Evaluation of T_e / T_g as function of b and L

$$\begin{aligned}\frac{T_e}{T_g} = & + 0.739\times 10^{0}\times 1 - 81.44\times 10^{0}\times b \\ & + 134.7\times 10^{0}\times L + 833.5\times 10^{0}\times b\times L \\ & + 3.345\times 10^{3}\times b^{2} - 31.25\times 10^{3}\times L^{2} \\ & - 201.6\times 10^{3}\times b^{2}\times L + 606.4\times 10^{3}\times b\times L^{2} \\ & - 62.69\times 10^{3}\times b^{3} + 3.160\times 10^{6}\times L^{3} \\ & + 2.300\times 10^{6}\times b^{2}\times L^{2} + 3.550\times 10^{6}\times b^{3}\times L \\ & - 52.00\times 10^{6}\times b\times L^{3} + 536.0\times 10^{3}\times b^{4} \\ & - 155.0\times 10^{6}\times L^{4} - 55.40\times 10^{6}\times b^{3}\times L^{2} \\ & + 101.0\times 10^{6}\times b^{2}\times L^{3} - 17.60\times 10^{6}\times b^{4}\times L \\ & + 1.280\times 10^{9}\times b\times L^{4} - 1.590\times 10^{6}\times b^{5} \\ & + 3.040\times 10^{9}\times L^{5}\end{aligned} \quad (3\text{-}7)$$

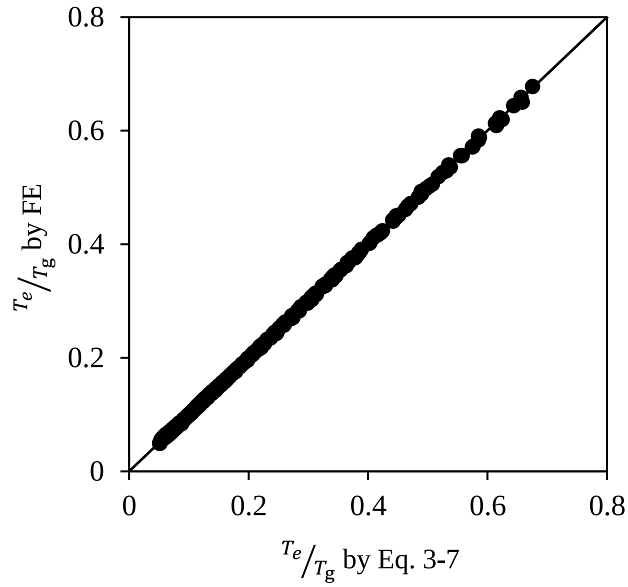

Figure 3-6: Accuracy of using Eq. 3-7 in predicting T_e / T_g

3.1.3 Validation

The experimental test conducted by Chen et al. [32] was utilized to validate the proposed heat transfer method. The test involved heating a 600 mm by 600 mm by 6 mm ordinary glass panel using a natural fire curve. The width of the protected part was 10 mm. Eq. 3-6 was first used to predict the temperature at the glass center. Afterward, $\frac{T_e}{T_g}$ was evaluated using Eq. 3-7 and found to be equal to 0.474. As shown in Fig. 3-7a, the results of the proposed approach are in good agreement with the experimental study. It should be noted that Eq. 3-7 is only valid after the ratio $\frac{T_e}{T_g}$ becomes constant, which is at about 250 second for this sample. However, the use of a constant ambient temperature for the duration before the 250 second seems to provide good results.

To further validate the proposed method, the experimental tests conducted by Harada et al. [11] and Zhao et al. [33] were considered. The glass panel dimensions were 500 mm by 500 mm by 3 mm and 600 mm by 600 mm by 6 mm, respectively. The width of the covered part was 15 mm and 10 mm, respectively. Figs. 3-7b and 3-7c show that the proposed approach predicted the temperature at the center and edge of the glass panels with good accuracy. The small differences between the experimental and numerical results can be due to experimental errors, or numerical assumptions including: (1) uniform temperature across the glass thickness, (2) constant glass thermal properties, and (3) ignoring radiation and convection for the covered part of the glass panel.

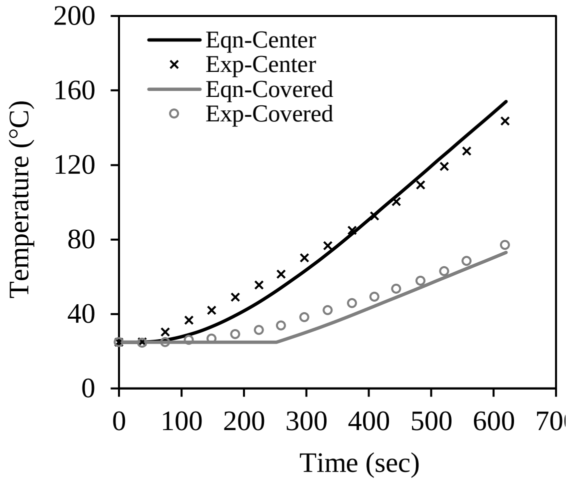

(a) Experimental by Chen et al. [32]

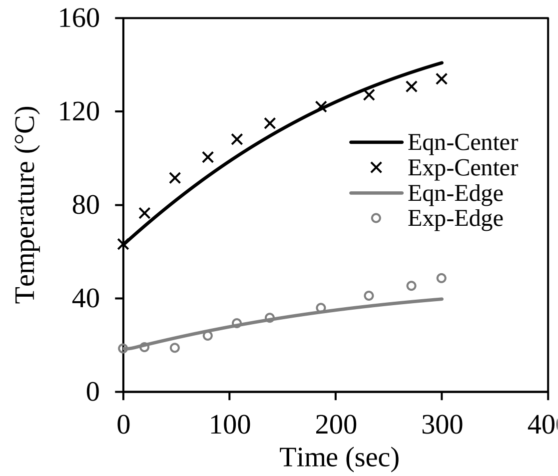

(b) Experimental by Harada et al. [11]

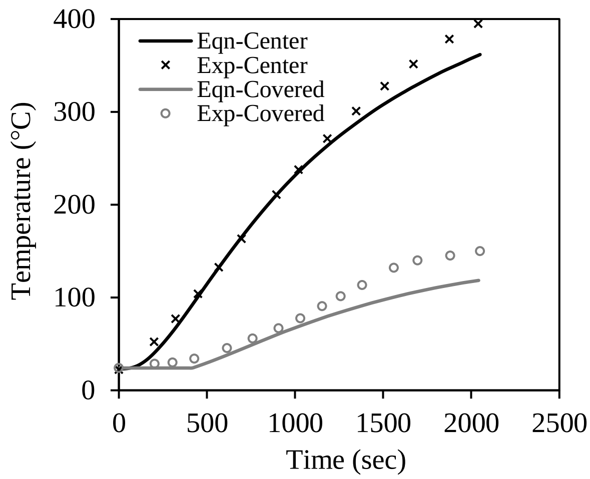

(c) Experimental by Zhao et al. [33]

Figure 3-7: Validation of the Proposed Approach

3.2 Maximum Developed Thermal Stress

The second step in the proposed approach is to determine the maximum developed thermal stress. The following subsections provide the development of a simplified method to estimate the maximum thermal stress, and then generalize the simplified method to be applicable for any temperature distribution.

3.2.1 Proposed simplified method

Fig. 3-8a shows a glass panel, with dimensions W by H, and a frame width b. The connection between the panel and the frame is assumed to have enough clearance to allow for free expansion [7,14,22]. During fire exposure, the temperature in the protected part is much lower than the temperature of the exposed part. The resulting unrestrained thermal strain distribution (ε_{th}) is shown in Fig. 3-8b. This free-thermal expansion cannot develop, as the glass is expected to follow the plane section assumption. Thus, a self-induced strain (ε_s), Fig. 3-8c, is expected to develop to convert the free thermal strain to an equivalent linear strain ($\overline{\varepsilon_{th}}$), which is uniform for the presented case because of the symmetry of the unrestrained thermal strains. The uniform strain, ε_i, shown in Fig. 3-8d reflects the actual deformation of the glass. This concept was previously adopted by El-Fitiany and Youssef [3], while analyzing reinforced concrete cross sections exposed to fire.

The self-induced strains must be in-self equilibrium. They can be divided into internal compressive strains (ε_{sc}) for the exposed glass area and tensile strains (ε_{st}) for the protected glass area (Fig. 3-8c). These tensile strains correspond to the maximum tensile stresses, which will develop in the glass sample.

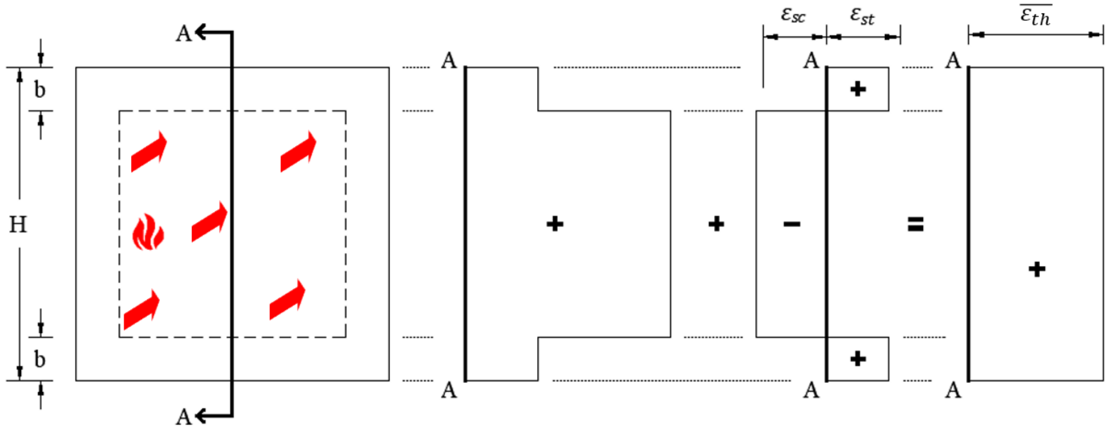

(a) Heated glass panel (b) ε_{th} (c) ε_s (d) $\overline{\varepsilon_{th}}$

Figure 3-8: Developed strains in uniformly heated glass panel

Eqs. 3-8 and 3-9 can be derived based on the uniform total strain and the equilibrium of the self-induced stresses.

$$\varepsilon_{st} + \alpha_g \times T_e = \alpha_g \times T_g - \varepsilon_{sc} \tag{3-8}$$

$$\varepsilon_{st} = \varepsilon_{sc}\left(\frac{H}{2b} - 1\right) \tag{3-9}$$

Where α_g is the glass thermal expansion coefficient. The value of the self-induced tensile thermal strain can then be obtained by solving Eqs. 3-8 and 3-9, which results in Eq. 3-10.

$$\varepsilon_{st} = \alpha_g(T_g - T_e)\left(1 - \frac{2b}{H}\right) \tag{3-10}$$

Eq. 3-10 indicates that the self-induced tensile strain increases with the increase of the height of the glass panel (H) and the difference in temperature between the exposed and protected regions. It decreases with the increase of width of the protected area (b). These findings are in agreements with the findings of previous experiments [15,22,34]. It should be noted that the factor $\left(1-\frac{2b}{H}\right)$ is consistent with the geometric factor proposed by Pagni [8,14], which was developed based on a hyperbolic temperature variation.

3.2.2 Generalization of the proposed simplified method

In a real fire scenario, the glass panel is expected to have a variable temperature profile. This section explores the use of the developed simplified method for the case of linearly varying temperature profile. The derivation, shown below, can be modified to accommodate other temperature distributions.

Fig. 3-9a shows a glass panel, exposed to higher average temperatures at its top than its bottom. The temperature within the width b was assumed to be constant with values T_{et} at the top and T_{eb} at the bottom. The temperature of the exposed region of the glass panel was assumed to be varying linearly from T_{gt} at the top to T_{gb} at the bottom. This linear temperature distribution considers the convection of compartment fires where the temperature of the upper layers of air is higher than the lower ones. The resulting unrestrained thermal strains (ε_{th}), Fig. 3-9b, are ε_{th-et} at the top covered region, ε_{th-eb} at the bottom covered region, ε_{th-gt} at the top of the exposed region, and ε_{th-gb} at the bottom of the exposed region. Self-induced strains (ε_s), Fig. 3-9c, are expected to be developed to maintain the linearity of the thermal profile. The equivalent linear strain profile ($\overline{\varepsilon_{th}}$) is expected to be variable in this case with a middle strain ε_i and a curvature ψ_i.

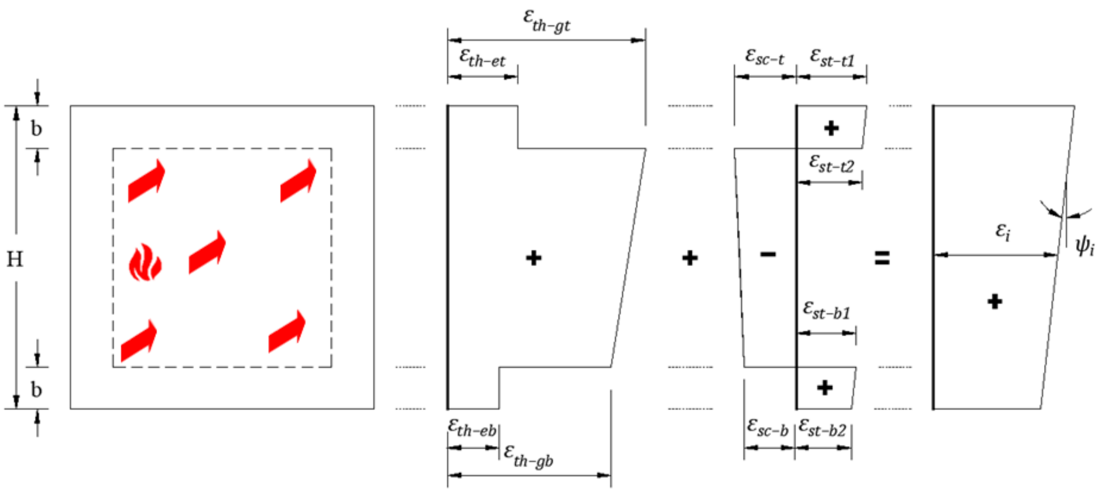

Figure 3-9: Developed strains in a glass panel heated at its top more than its bottom

The self-induced thermal strains can be expressed in terms of the equivalent thermal strains and the unrestrained thermal strains using the following equations.

$$\varepsilon_{st-t1} = \varepsilon_i + \psi_i \frac{\mathrm{H}}{2} - \varepsilon_{th-et} \tag{3-11a}$$

$$\varepsilon_{st-t2} = \varepsilon_i + \psi_i \frac{\mathrm{H} - 2\mathrm{b}}{2} - \varepsilon_{th-et} \tag{3-11b}$$

$$\varepsilon_{st-b1} = \varepsilon_i - \psi_i \frac{\mathrm{H} - 2\mathrm{b}}{2} - \varepsilon_{th-eb} \tag{3-11c}$$

$$\varepsilon_{st-b2} = \varepsilon_i - \psi_i \frac{\mathrm{H}}{2} - \varepsilon_{th-eb} \tag{3-11d}$$

$$\varepsilon_{sc-t} = \varepsilon_i + \psi_i \frac{H - 2b}{2} - \varepsilon_{th-gt} \tag{3-11e}$$

$$\varepsilon_{sc-b} = \varepsilon_i - \psi_i \frac{\mathrm{H} - 2\mathrm{b}}{2} - \varepsilon_{th-gb} \tag{3-11f}$$

Where ε_{st-t1}, ε_{st-t2}, ε_{st-b1} and ε_{st-b2} are the self-induced tensile strains at the top and bottom edges of the covered areas as demonstrated in Fig. 3-9c. ε_{sc-t} and ε_{sc-b} are the self-induced compressive strains at the top and bottom of the exposed part of the glass.

Eqs. 3-12 and 3-13 can then be derived based on equilibrium of forces and moments resulting from the self-induced strains.

$$\varepsilon_i = \frac{\alpha_g \mathrm{b}}{\mathrm{H}}(T_{et} + T_{eb}) + \frac{\alpha_g(\mathrm{H} - 2\mathrm{b})}{2\mathrm{H}}\left(T_{gt} + T_{gb}\right) \tag{3-12}$$

$$\psi_i = \frac{\alpha_g(6bH - 6b^2)}{H^3}(T_{et} - T_{eb}) + \frac{\alpha_g(H - 2b)^2}{H^3}\left(T_{gt} - T_{gb}\right) \tag{3-13}$$

3.3 Validation

The proposed approach is used to calculate the tensile stress generated during fire exposure of different glass panels given in the literature. Table 3-1 provides a summary of the validation cases. Wang et al. [22] experimentally tested ordinary glass panels with dimensions of 300 mm by 300 mm by 6 mm, which were protected at the edges by a frame width of 20 mm. The glass panel was heated in a small air compartment using a heating panel. The heating rate was 10 ºC/min until the air reached a temperature of 600 ºC, which was kept constant for a period of 20 minutes. Harada et al. [11] exposed ordinary glass panels to heat fluxes ranging between 2.7 kW/m^2 and 9.7 kW/m^2. The size of the glass panels was 500 mm by 500 mm by 3 mm and they were protected at the edges by a frame width of 15 mm. Wang et al. [35] developed a finite element program to investigate the thermal stress distribution during fire exposure. The program was validated using the experiments by Skelly et al. [36] on ordinary glass panel exposed to pool fire. The analyzed glass panels had a size of 500 mm by 280 mm by 2.4 mm and the width of the supporting frame was 25 mm. Chen et al. [15] exposed ordinary glass panels to radiant heating in an enclosed compartment. The glass panel size was 600 mm by 600 mm by 6 mm and the width of the frame was 30 mm. The measured temperature field was implemented into a finite element program developed by the authors to predict the resultant stresses. Dembele et al. [19] developed a program (Glaz3D) that was validated with ANSYS [37] to study the thermal and mechanical behavior of glazing elements during fire. The validation results are summarized in Fig. 3-10. As shown in the figure, the proposed approach predicted the fracture tensile strength with an accuracy of ±10%.

Table 3-1: Validation cases

Parameter	Reference				
	[22]	**[11]**	**[35]**	**[15]**	**[19]**
E, (10^{10} Pa)	6.7	7.3	7.0	6.72	7.3
α_g, (10^{-6} K^{-1})	8.5	8.75	8.5	8.46	8.75
Glass panel size, (m^2)	0.3 × 0.3	0.5 × 0.5	0.50 × 0.28	0.6 × 0.6	0.3 × 0.3
Thickness, L (m)	0.006	0.003	0.0024	0.006	0.003
Covered part, b, (m)	0.02	0.015	0.025	0.03	0.015
Max. temperature difference (ºC)	67 – 150	17 – 70	143	133	80

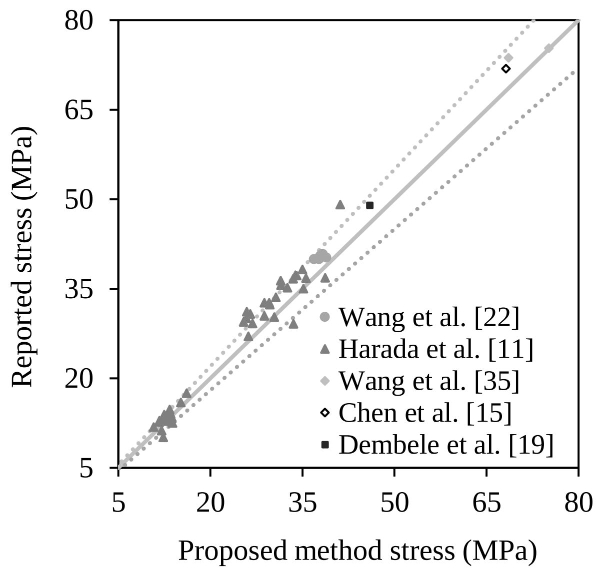

Figure 3-10: Validation results

3.4 Conclusion

This chapter provides a simple yet reliable approach to assess the behavior of ordinary glass panels during fire exposure. A set of simplified methods were developed to conduct both heat transfer and stress calculations.

For heat transfer calculations, a simplified method to estimate the temperature at the center of the glass panel was proposed. The method assumes that the temperature across the glass thickness is constant. The finite element method was then utilized to develop an equation that relates the temperature at the edge of the panel to the temperature at its center. For stress calculations, a simplified method to estimate the self-induced thermal strains, which maintain the plane section assumption, is developed considering cases of uniform fire exposure and non-uniform fire exposure. Predictions of the proposed approach were compared to the experimental and numerical work by others. The comparisons have confirmed the accuracy of the proposed approach in estimating the maximum tensile stress developed during fire exposure.

3.5 References

[1] R.T. Kuehnen, M.A. Youssef, Equivalent Standard Fire Duration to Evaluate Internal Temperatures in Natural Fire Exposed RC Beams, Fire Safety Journal 108 (2019) 102831. doi:10.1016/j.firesaf.2019.102831.

[2] S.F. El-Fitiany, M.A. Youssef, Interaction diagrams for fire-exposed reinforced concrete sections, Engineering Structures. 70 (2014) 246–259. doi:10.1016/j.engstruct.2014.03.029.

[3] S.F. El-Fitiany, M.A. Youssef, Assessing the flexural and axial behaviour of reinforced concrete members at elevated temperatures using sectional analysis, Fire Safety Journal 44 (2009) 691–703. doi:10.1016/j.firesaf.2009.01.005.

[4] S.F. El-Fitiany, M.A. Youssef, Simplified method to analyze continuous reinforced concrete beams during fire exposure, ACI Struct. J. 111 (2014) 145–155. doi:10.14359/51686544.

[5] H.W. Emmons, The needed fire science, in: Fire Safety Science First International Symposium, IAFSS, 1986: pp. 33–53.

[6] K. Nguyen, P. Weerasinghe, P. Mendis, T. Ngo, J. Barnett, Performance of modern building facades in fire: a comprehensive review, Electronic Journal of Structural Engineering 16 (2016) 69–86.

[7] O. Keski-rahkonen, Breaking of Window Glass Close, Fire Technology 12 (1988) 61–69.

[8] P.J. Pagni, A.A. Joshi, Glass Breaking In Fires, Fire Safety Science 3 (1991) 791–802. doi:10.3801/IAFSS.FSS.3-791.

[9] C. Bedon, Structural Glass Systems under Fire: Overview of Design Issues, Experimental Research, and Developments, Adv. Civ. Eng. 2017 (2017). doi:10.1155/2017/2120570.

[10] A.A. Joshi, P.J. Pagni, Fire-induced thermal fields in window glass. II—Experiments, Fire Safety Journal 22 (1994) 45–65. doi:10.1016/0379-7112(94)90051-5.

[11] K. Harada, A. Enomoto, K. Uede, T. Wakamatsu, An experimental study on glass cracking and fallout by radiant heat exposure, Fire Safety Science (2000) 1063–1074. doi:10.3801/IAFSS.FSS.6-1063.

[12] T.J. Shields, G.W.H. Silcock, M.F. Flood, Performance of a single glazing assembly exposed to enclosure corner fires of increasing severity, Fire Mater. 25 (2001) 123–152. doi:10.1002/fam.764.

[13] T.J. Shields, G.W.H. Silcock, M.F. Flood, Performance of a single glazing assembly exposed to a fire in the centre of an enclosure, Fire Mater. 26 (2002) 51–75. doi:10.1002/fam.783.

[14] P.J. Pagni, Thermal glass breakage, Fire Safety Science (2003) 3–22. doi:10.3801/IAFSS.FSS.7-3.

[15] H. Chen, Q. Wang, Y. Wang, H. Zhao, J. Sun, L. He, Experimental and Numerical Study of Window Glass Breakage with Varying Shaded Widths under Thermal Loading, Fire Technology 53 (2017) 43–64. doi:10.1007/s10694-016-0596-0.

[16] Y. Yang, C.L. Chow, Transient temperature fields and thermal stress fields in glazing of different thicknesses exposed to heat radiation, Construction and Building Materials 193 (2018) 589–603. doi:10.1016/j.conbuildmat.2018.10.106.

[17] Y. Wang, Q. Wang, G. Shao, H. Chen, Y. Su, J. Sun, L. He, J.X. Wen, R. Zong, K.M. Liew, Experimental study on thermal breakage of four-point fixed glass façade, Fire Safety Science 11 (2014) 666–676. doi:10.3801/IAFSS.FSS.11-666.

[18] A. Vedrtnam, C. Bedon, M.A. Youssef, M. Wamiq, A. Sabsabi, S. Chaturvedi, Experimental and numerical structural assessment of transparent and tinted glass during fire exposure, Construction and Building Materials 250 (2020). doi:10.1016/j.conbuildmat.2020.118918.

[19] S. Dembele, R.A.F. Rosario, J.X. Wen, Thermal breakage of window glass in room fires conditions - Analysis of some important parameters, Build. Environ. 54 (2012) 61–70. doi:10.1016/j.buildenv.2012.01.009.

[20] C. Bedon, C. Louter, Thermo-mechanical Numerical Modelling of Structural Glass under Fire - Preliminary Considerations and Comparisons, (2018). doi:10.7480/cgc.6.2173.

[21] M. Kozlowski, C. Bedon, D. Honfi, Numerical analysis and 1D/2D sensitivity study for monolithic and laminated structural glass elements under thermal exposure, Materials (Basel). 11 (2018). doi:10.3390/ma11081447.

[22] Y. Wang, Y. Zhang, Q. Wang, Y. Yang, J. Sun, The effect of glass panel dimension on the fire response of glass façades, Construction and Building Materials 181 (2018) 588–597. doi:10.1016/j.conbuildmat.2018.06.088.

[23] Y. Yang, L. Miao, C.L. Chow, Relative significance of temperature gradient components on cracking behavior in glass panes under thermal radiation, Appl. Therm. Eng. 131 (2018) 837–848. doi:10.1016/j.applthermaleng.2017.12.060.

[24] Y. Wang, Q. Wang, Y. Su, J. Sun, L. He, K.M. Liew, Fracture behavior of framing coated glass curtain walls under fire conditions, Fire Safety Journal 75 (2015) 45–58. doi:10.1016/j.firesaf.2015.05.002.

[25] W. Lu, Y. Wang, H. Chen, L. Jiang, Q. Duan, M. Li, Q. Wang, J. Sun, Investigation of the thermal response and breakage mechanism of point-supported glass facade under wind load, Construction and Building Materials 186 (2018) 635–643. doi:10.1016/j.conbuildmat.2018.07.114.

[26] D. Drysdale, An introduction to fire dynamics, 3rd ed., John Wiley & Sons, Hoboken, N.J, 2011.

[27] F.P. Incropera, D.P. Dewitt, T.L. Bergman, D.S. Lavine, Fundanmentals of Heat and Mass Hransfer, 6th ed., John Wiley, Hoboken, NJ, 1993.

[28] J.P. Holman, Heat transfer, 10th ed., McGraw Hill Higher Education, Boston, 2010.

[29] Y. Wang, J. Hu, Performance of laminated glazing under fire conditions, Compos. Struct. 223 (2019). doi:10.1016/j.compstruct.2019.110903.

[30] Dassault Systemes Simulia, Abaqus 6.14 documentation, Provid. Rhode Island, US. (2017).

[31] International Organization for Standards, ISO 834 - Fire Resistance Tests – Elements of Building Construction, Geneva, Switzerland, 2014.

[32] H. Chen, H. Zhao, Y. Wang, Q. Wang, J. Sun, The Breakage of Float Glass with Four-Edge Shading Under the Combined Effect of Wind Loading and Thermal Loading, Fire Technology 53 (2017) 1233–1248. doi:10.1007/s10694-016-0630-2.

[33] H. Zhao, Q. Wang, Y. Su, Y. Wang, G. Shao, H. Chen, J. Sun, Experimental Investigation on Glass Cracking for Wind Load Combined with Radiant Heating, in: Fire Sci. Technol. 2015, Springer, 2017: pp. 255–260.

[34] A.A. Joshi, P.J. Pagni, Fire-Induced Thermal Fields in Window Glass . I—Theory, 22 (1994) 25–43.

[35] Q. Wang, Y. Zhang, Y. Wang, J. Sun, L. He, Dynamic three-dimensional stress prediction of window glass under thermal loading, Int. J. Therm. Sci. 59 (2012) 152–160. doi:10.1016/j.ijthermalsci.2012.03.018.

[36] M.J. Skelly, R.J. Roby, C.L. Beyler, Experimental investigation of glass breakage in compartment fires, J. Fire Prot. Eng. 3 (1991) 25–34. doi:10.1177/104239159100300103.

[37] ANSYSInc., ANSYS CFX-Solver, release 10.0, (2005).

Chapter 4

4 Simplified Structural Analysis of Laminated Glass Panels during Fire Exposure

During the service life of a building, the risk of experiencing a fire event is very high. If such a fire is left to develop, the losses are expected to be tremendous. The availability of fuel sources and oxygen are the two main factors that affect the development of a fire [1]. The latter is directly related to the presence of openings in the building's envelope (e.g., broken glass in building façade). Therefore, to delay the development of the fire, glass must stay intact to provide a barrier, which limits the oxygen supply and prevents the spreading of flames and smoke to unaffected areas. Current literature sufficiently covers the fire performance of the construction materials typically used in structural elements such as concrete, masonry, and steel [2–6]. However, it is also crucial to have an in-depth knowledge of the performance of glass under elevated temperatures to guarantee adequate fire performance while avoiding unnecessarily extra costs associated with using overly designed glass assemblies.

Glass is a brittle material that has low fire resistance due to its susceptibility to failure from thermal shock [7,8]. Ordinary glass (e.g., float glass) has the lowest cost as compared to other types of glass and is commonly used in residential buildings. However, it has the lowest strength and fire resistance. Other types of glass with improved properties (e.g., toughened glass) have a higher structural capacity. However, their post-breakage behavior (e.g., shatter when broken) is undesirable for fire safety requirements. Wired glass has been commonly used in locations where fire safety glass is required by building codes. Should failure of wired glass occur, broken glass pieces would be held by the wire preventing the formation of an opening. However, the addition of the wire reduces the impact resistance of the glass as it increases the number of flaws [9].

Laminated glass could be an optimum choice that provides the desired fire safety requirements (e.g., post-breakage integrity) without compromising the structural capacity. This type of glass is manufactured by permanently bonding two or more glass panels with bonding layers [10]. When cracked, broken glass pieces adhere to the interlayers through shear interaction [11]. This chapter summarizes the existing research on laminated glass during fire exposure and proposes a new method to determine the temperature of the glass during fire exposure and the corresponding maximum thermal stress.

The post-breakage behavior of laminated glass assembly varies depending on the type of glass panels and interlayer material (Fig. 4-1). Polyvinyl Butyral (PVB) is the most common type of interlayer materials. However, other materials can be used such as Ethylene-Vinyl Acetate (EVA) or SentryGlas® (SG) [12]. The standard thicknesses of the interlayer are 0.38 mm, 0.76 mm, 1.52 mm, 2.28 mm, and 3.04 mm [13]. PVB is a viscoelastic material. Therefore, its physical properties are highly dependent on the temperature and the load duration [9]. The interlayer causes the broken glass pieces to arch and/or lock, which make them intact.

The glass panels, that are used in the lamination process, can be ordinary float glass, heat-strengthened glass, toughened glass, or a combination of those types. Depending on the used type, the post-breakage behavior of the assembly changes. Laminated glass, which is composed of toughened glass panels, is susceptible to shattering into highly fragmented pieces, and, therefore, it does not provide any post-breakage stability. The PVB interlayer tends to tear, causing large deformations that can lead to the glass sliding out from its supports and eventually collapse [9].

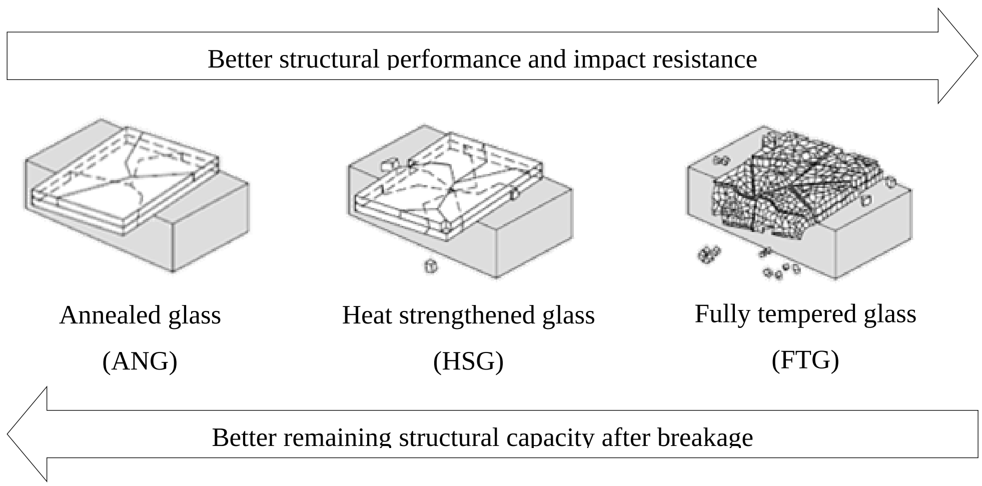

Figure 4-1: Post breakage behavior of laminated glass

To the author's knowledge, the behavior of laminated glass panels during fire exposure has not been extensively discussed in the literature and practical and reliable methods that can be used to predict the behavior of laminated glass during fire are scarce. The following sections provides details about the proposed method to estimate the temperature and the maximum thermal stress of laminated glass panels during fire exposure. Although, the developed methods assume two ordinary glass panels connected with a PVB interlayer, they can be extended to cover other types of laminated glass.

4.1 Temperature of Laminated Glass during Fire Exposure

In this section, a simplified approach is developed to predict the temperature at the center and edge of each of the laminated glass panels during fire exposure. The approach starts by utilizing the heat transfer equation (Eq. 3-6), proposed in Chapter 3, to determine the temperature at the interlayer, and, then uses this temperature to evaluate the temperature gradient across the thickness of the exposed part of the two assumed glass panels. The temperature of the covered part of each of the glass panels is then calculated as a function of the evaluated temperatures.

4.1.1 Temperature of the interlayer at the exposed part of the glass

Given that the thickness of the interlayer is very small as compared to the thickness of the glass panels and that the drop in temperature within the interlayer diminishes during fire exposure [15], the temperature within the interlayer can be assumed to be constant and equal to the attached faces of the glass panels.

To further illustrate the effect of the interlayer on the heat distribution in laminated glass exposed to fire, the commercial software ABAQUS [16] was utilized to calculate the temperature distribution for a case study sample. The experimental study sample was assumed to have dimensions of 500 mm by 500 mm by 12.38 mm (two-6 mm glass panels and 0.38 mm PVB Interlayer) and was supported at its edges by a frame, which is covering 20 mm of the panel. It was exposed for 30 minutes to ISO 834 temperature-time relationship [17]. The sample was modeled using the 8-node-3D linear-heat transfer brick elements (DC3D8 type from ABAQUS library). A maximum mesh size of 10 mm was found to result in acceptable accuracy, and, thus was utilized. The generated mesh is shown in Fig. 4-2a. The fire was applied as uniform surface interaction (i.e., radiation and convection) on the exposed glass surface, surface S1 in Fig. 4-2b. Where L_g and L_{PVB} are the thicknesses of the glass panels and PVB, respectively. Heat losses were assumed to only occur on the opposite glass surface (side S4), which is exposed to ambient temperature. The material properties for the glass and the PVB for the modeled panels are given in Table 4-1 [15]. Fig. 4-3 shows the change in temperature gradients across the glass thickness with time. As shown in the figure, the temperature drops within the interlayer is very small as compared to the drop in temperature within the glass and this drop becomes less significant with time (i.e. increased temperature). These obtained results justify the simplification of assuming a constant temperature with the interface layer.

Table 4-1: Glass and PVB properties

Parameter	**Symbol**	**Value**	**Unit**
Glass			
Density	ρ	2500	kg/m^3
Specific Heat	c	720	J/kg·K
Thermal Conductivity	λ	0.94	W/m·K
Emissivity	ε	0.85	–
PVB			
Density	ρ_{PVB}	1070	kg/m^3
Specific Heat	c_{PVB}	1100	J/kg·K
Thermal Conductivity	λ_{PVB}	0.221	W/m·K
Ambient Temperature (T_i) = 20°C			

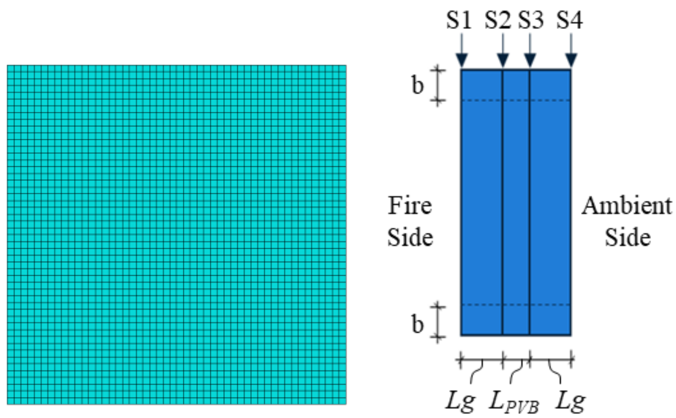

(a) Generated Mesh (b) Cross Section View

Figure 4-2: Simulation of Laminated Glass Panel using ABAQUS

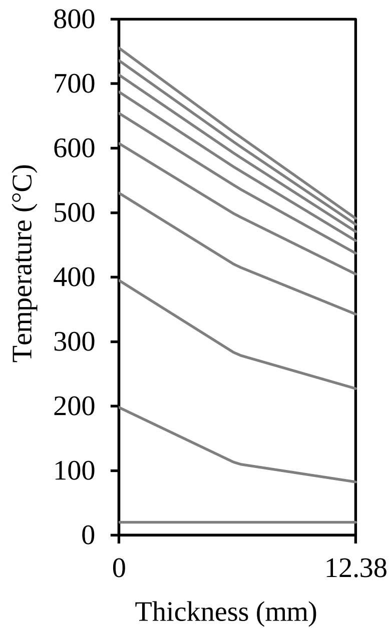

Figure 4-3: Temperature gradients across thickness with time

An approach to determine the temperature of monolithic glass panels (T_g) during fire exposure was previously proposed by Sabsabi et al. [14]. Eq. 4-1 was utilized to determine the temperature at the middle of the exposed part of the glass thickness considering both standard and natural fire curves. For laminated glass, it is proposed to utilize the same approach to calculate the average temperature of the interlayer.

$$\Delta T = \frac{\Delta t}{\rho c L}\left[h_f\left(T_\infty - T_g\right) + \varepsilon\sigma\left({T_\infty}^4 - {T_g}^4\right) - h_b\left(T_g - T_i\right) - \varepsilon\sigma\left({T_g}^4 - {T_i}^4\right)\right] \qquad (4\text{-}1)$$

Where L is the total thickness of the laminated glass panel, T_∞ is the temperature of the fire, Δt is the time increment, ρ is the glass density, c is the glass specific heat, ε is the emissivity of the glass and can be assumed equal to 0.85 [15], σ is the Stefan–Boltzmann constant, h_f and h_b are the film coefficients at the fire and ambient sides, respectively, and can be defined using Eq. 3-2. Fig. 4-4 shows the accuracy of Eq. 4-1 in calculating the average temperature of the interlayer compared to the results from ABAQUS considering the glass panel described earlier in this section and considering two thicknesses for the laminated glass (10.38 mm and 32.28 mm). The figure shows that the error in predicting this average temperature increases with the increase of glass thickness. However, the maximum error (less than 15%) for the extreme case of two glass panels, each with 15 mm thickness, and PVB interlayer thickness of 2.28 mm is still within reasonable limits (Fig. 4-4b).

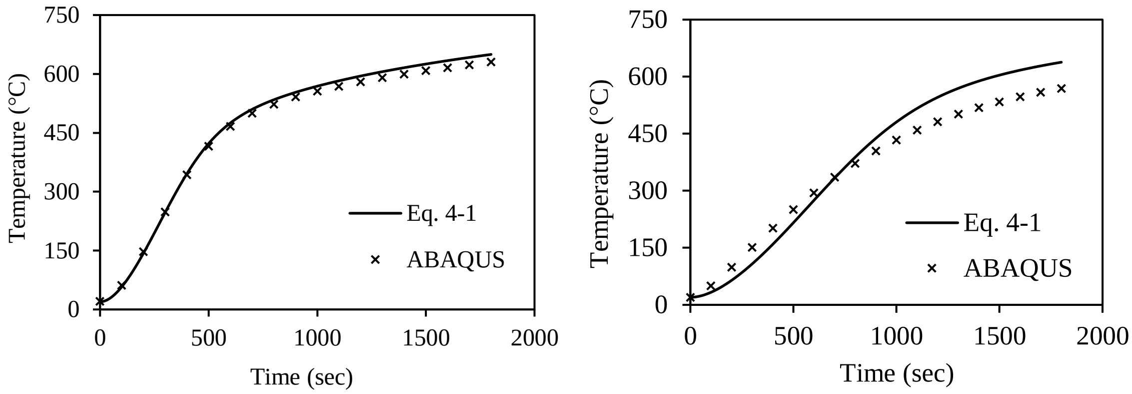

(a) Laminated glass sample with total thickness of 10.38 mm

(b) Laminated glass sample with total thickness of 32.28 mm

Figure 4-4: Average temperature of interlayer

4.1.2 Temperature across the glass thickness

A parametric study was conducted using the commercial software ABAQUS [16] to determine the ratio between the average temperature of the interlayer (T_g) and the temperature of the ambient side (T_{gb}), S4, as well as the temperature of the fire side (T_{gf}), S1. Heating of the exposed part of the glass, Fig. 4-2b, was simulated as uniform surface interaction that involved radiation and convection. For such a case, the change in the glass dimensions do not affect the calculated ratios. The only parameters that need to be considered are the glass thickness (L_g), the PVB thickness (L_{PVB}), and the fire scenario. The thicknesses of glass and PVB layers were assumed to range from 5 mm to 15 mm and 0.38 to 2.28 mm, respectively. These ranges deemed to cover most of the practical values available in the literature. The glass panels were assumed to be exposed to ISO 834 temperature-time relationship [17]. The same model properties used in the previous section were used for this parametric study. The temperatures at the fire side and ambient sides

(Fig. 4-2b) were recorded for each run. Sample for the obtained variation of $\frac{T_{gb}}{T_g}$ with time, as produced by ABAQUS, is shown in Fig. 4-5.

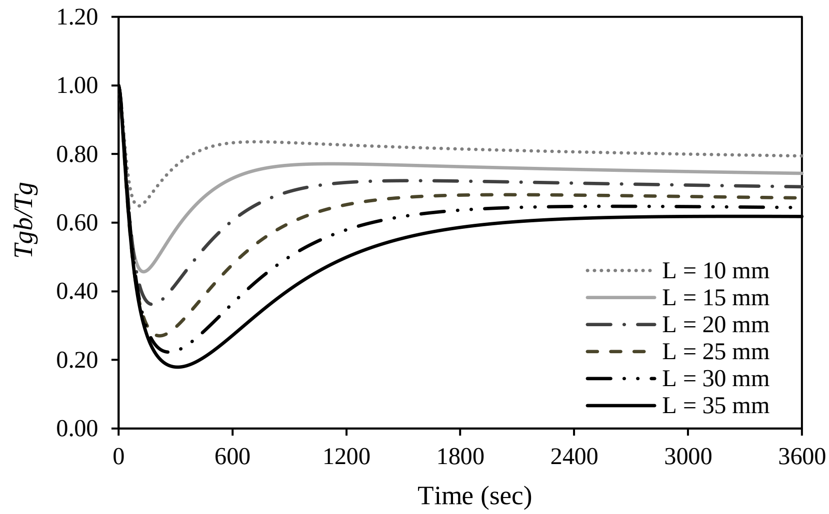

Figure 4-5: Variation of T_{gb} / T_g with time

Initially, the entire glass assembly had the same temperature. As the time (fire temperature) increases, the ratio between the center and back temperature keeps decreasing until reaching its lowest value after a time t_{min}. Afterwards, the ratio starts increasing until reaching a constant value. The value of t_{min} increases with increase of the glass thickness as more time would be needed to heat the back side of the panel. t_{min} in seconds can be calculated using Eq. 4-2.

$$t_{min} = 8502.9\, L\ (\text{m}) + 8.38 \qquad (4\text{-}2)$$

Figure 4-7 can be easily used by engineers to determine the temperature distribution across the glass panel by utilizing the average temperature of the interlayer and assuming a linear temperature distribution. To further simplify calculation of $\frac{T_{gb}}{T_g}$, the figure data were utilized to develop the formula given by Eq. 4-3, which allow calculating the ratio as function of time, *t* (sec), and *L* (m). The equation and coefficients were determined using a least square regression analysis, common regression requirements of probability (p) < 0.0001 and correlation (R^2_{adj}) > 95% were maintained. Knowing Tg and Tgb, the temperature of the exposed face can then be linearly extrapolated. The maximum error associated with using Eq. 4-3 is less than 10%, as shown in Fig. 4-6.

$$\frac{T_{gb}}{T_g} = \mathrm{A} + \mathrm{B}L + \mathrm{C}t + \mathrm{D}Lt + \mathrm{E}L^2 + \mathrm{F}t^2 + \mathrm{G}L^3 + \mathrm{H}t^3 + \mathrm{I}L^2t^2 + \mathrm{J}L^4 + \mathrm{K}t^4 + \mathrm{M}L^3t^2 + \mathrm{N}L^2t^3 + \mathrm{O}L^5 + \mathrm{P}t^5 \tag{4-3}$$

Table 4-2: Coefficients for Eq. (4-3)

Range		$t \le t_{min}$			$t > t_{min}$		
Coefficients	A	+	4.738×	10^0	+	1.182×	10^0
	B	−	0.954×	10^3	−	94.82×	10^0
	C	−	4.949×	10^{-3}	+	0.610×	10^{-3}
	D	−	0.120×	10^0	+	22.47×	10^{-3}
	E	+	93.03×	10^3	+	4.647×	10^3
	F	−	5.052×	10^{-6}	−	0.789×	10^{-6}
	G	−	4.368×	10^6	−	177.7×	10^3
	H	+	0.373×	10^{-6}	+	0.349×	10^{-9}
	I	−	16.55×	10^{-3}	−	0.255×	10^{-3}
	J	+	99.23×	10^6	+	3.623×	10^6
	K	−	1.489×	10^{-9}	−	0.072×	10^{-12}
	M	+	0.749×	10^0	+	3.181×	10^{-3}
	N	−	55.00×	10^{-6}	+	12.11×	10^{-9}
	O	−	874.3×	10^6	−	31.47×	10^6
	P	+	2.087×	10^{-12}	+	5.776×	10^{-18}

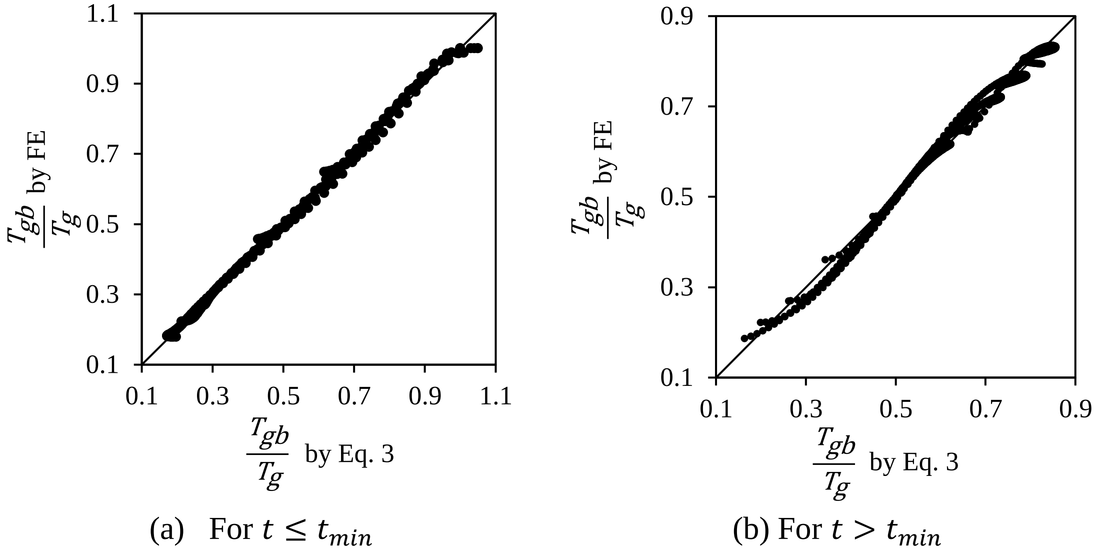

Figure 4-6: Accuracy of using Eq. 4-3 in predicting T_{gb} / T_g

4.1.3 Temperature at the edge of the glass panel

The temperature of the glass covered by the supporting frame is conservatively assumed to be completely protected from the direct effect of the fire, i.e. not affected by radiation and convection of the flames. Therefore, it is only heated through conduction from the exposed part. This concept was previously adopted by Sabsabi et al. [14] for ordinary glass panels during fire exposure. Sabsabi et al. [14] proposed a method to determine the temperature of the glass edge in terms of the temperature of the exposed part (T_g). The method assumes that the increase in temperature of the part covered by the frame (T_e) is only through conduction from the exposed center. This assumption reduces the complexity of the heat transfer problem and allows for an easy approximation for the edge temperature utilizing Eq. 3-6. The method was originally developed for monolithic glass sections, but it can still be utilized for laminated glass sections. However, it will need to be applied twice for each of the two glass panels.

4.1.4 Validation

The experimental test conducted by Wang and Hu [15] was utilized to validate the proposed heat transfer method. The test involved exposing a laminated glass panel (two 600 mm by 600 mm by 6 mm ordinary glass panels with 0.38 mm PVB layer in-between) to a natural fire curve. The width of the protected part was 20 mm. Eq. 4-1 was first used to predict the average temperature of the interlayer. Afterward, the change in T_{gb} at the ambient side (S4) and T_{gf} at the fire side (S1) with time were evaluated using Eq. 4-3. Finally, the temperature of the covered part was evaluated using Eq. 3-7. As shown in Fig. 4-7, the results of the proposed approach are in good agreement with the experimental results.

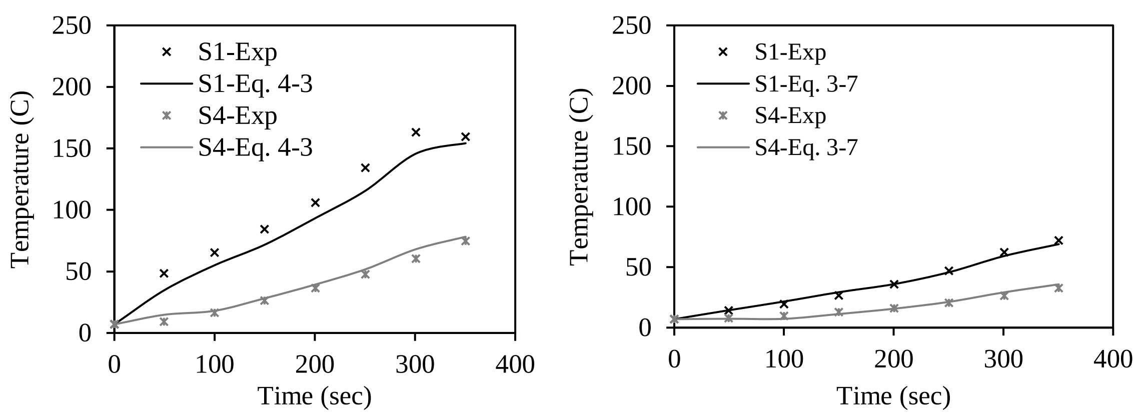

(a) Exposed part temperature (b) Covered part temperature

Figure 4-7: Validation of the proposed method

4.2 Maximum Developed Thermal Stress

During fire exposure, the exposed glass panel experiences the highest average temperature and conducts heat to the interlayer and the second panel. Consequently, the temperature distribution across the thickness would not be uniform, and each of the glass panels will experience different values of unrestrained thermal expansion (Fig. 4-9a). Two extreme cases can be assumed. They are related to the shear stiffness of the interlayer. If this stiffness is extremely high, the two glass panels act as a single monolithic section. On the other hand, if the shear stiffness is extremely low, each of the glass panels will act independently. The actual behavior can fall anywhere in-between these two bounds.

Fig. 4-9a shows the general case of n number of glass panels separated by m number of interlayers. Derivations are made for this general case. Assuming a higher shear stiffness for the interlayer, the concept of plane section remains plane needs to be applied to the whole assembly. The final strain distribution (Fig. 4-9b), ε, will consist of a uniform strain component, ε_e, and a curvature component, ψ_e (Figs. 4-9c and 4-9d).

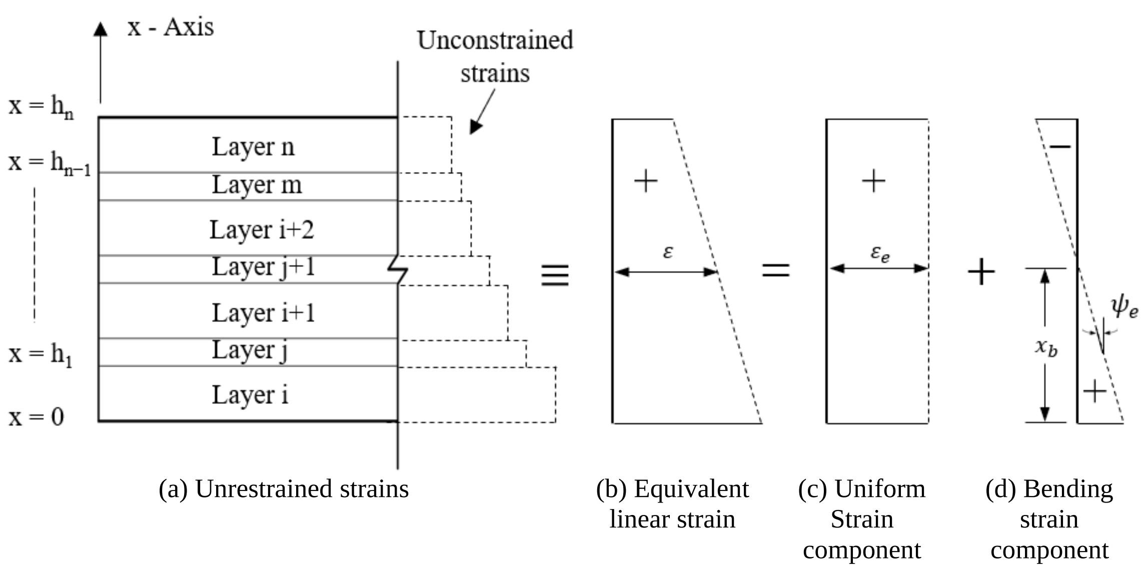

Figure 4-8: Developed strains across laminated glass with stiff interlayers

The conversion from the actual unrestrained thermal strain distribution to the equivalent linear distribution, ε, induces self-equilibrating internal stresses in the glass panels ($\varepsilon_{s,i}$) and in the interlayer ($\varepsilon_{s,j}$). The self-induced strains can be determined by calculating the difference between the assumed linear strain distributions and the unrestrained thermal strains

$$\varepsilon_{s,i} = \varepsilon - \varepsilon_{th,i} = \varepsilon - \alpha_i \Delta T_i \tag{4-4a}$$

$$\varepsilon_{s,j} = \varepsilon - \varepsilon_{th,j} = \varepsilon - \alpha_j \Delta T_j \tag{4-4b}$$

Where α_i & α_j, and ΔT_i & ΔT_j are coefficients of thermal expansion and the temperature change for the glass panels and interlayers, respectively.

ε can be divided to a uniform strain component and a bending strain component

$$\varepsilon = \varepsilon_e + \psi_e (x - x_b) \tag{4-5}$$

ε_e and the distance to the neutral axis x_b can be calculated from the force equilibrium (Eqs. 4-6a and 4-6b), which results in Eqs. 4-7 and 4-8.

$$\sum_{i=1}^{n} E_i(\varepsilon_e - \alpha_i \Delta T_i) t_i + \sum_{j=1}^{n-1} E_j(\varepsilon_e - \alpha_j \Delta T_j) t_j = 0 \tag{4-6a}$$

$$\sum_{i=1}^{n} \int_{h_{2i-2}}^{h_{2i-1}} \psi_e E_i (x - x_b)\, dx + \sum_{j=1}^{n-1} \int_{h_{2j-1}}^{h_{2j}} \psi_e E_j (x - x_b)\, dx = 0 \tag{4-6b}$$

$$\varepsilon_e = \frac{\sum_{i=1}^{n} \alpha_i E_i t_i \Delta T_i + \sum_{j=1}^{n-1} \alpha_j E_j t_j \Delta T_j}{\sum_{i=1}^{n} E_i t_i + \sum_{j=1}^{n-1} E_j t_j} \tag{4-7}$$

$$x_b = \frac{\sum_{i=1}^{n} E_i (h_{2i-1}^2 + h_{2i-2}^2) + \sum_{j=1}^{n-1} E_j (h_{2j}^2 + h_{2j-1}^2)}{2\left(\sum_{i=1}^{n} E_i t_i + \sum_{j=1}^{n-1} E_j t_j\right)} \tag{4-8}$$

Furthermore, from the moment equilibrium (Eq. 4-9), ψ_e can be calculated.

$$\sum_{i=1}^{n}\int_{h_{2i-2}}^{h_{2i-1}} E_i \varepsilon_{s,i}(x - x_b)\,dx + \sum_{j=1}^{n-1}\int_{h_{2j-1}}^{h_{2j}} E_j \varepsilon_{s,j}(x - x_b)\,dx = 0 \tag{4-9}$$

$$\psi_e = \frac{-3\left[\sum_{i=1}^{n} E_i(\varepsilon_e + \alpha_i \Delta T_i)(h_{2i-1}^2 + h_{2i-2}^2) + \sum_{j=1}^{n-1} E_j\left(\varepsilon_e + \alpha_j \Delta T_j\right)\left(h_{2j}^2 + h_{2j-1}^2\right)\right]}{\sum_{i=1}^{n} E_i[2(h_{2i-1}^3 + h_{2i-2}^3) - 3x_b(h_{2i-1}^2 + h_{2i-2}^2)] - \sum_{j=1}^{n-1} E_j\left[2\left(h_{2j}^3 + h_{2j-1}^3\right) - 3x_b\left(h_{2j}^2 + h_{2j-1}^2\right)\right]} \tag{4-10}$$

Eqs. 4-4a and 4-4b can be used to calculate the self-induced strains caused by the temperature gradients across the glass assembly thickness.

It is crucial to understand the behavior of the PVB-interlayer at elevated temperatures to be able to determine the overall behavior of the glass assembly. Haldimann et al. [9] suggested that at temperatures well below 0 ºC and for short duration loads, PVB is able to transfer the full shear stress from one panel of glass to another. On the other hand, for higher temperatures and long duration loads, the shear transfer is greatly reduced. Behr et al. [18] indicated that the performance of laminated glass with polyvinyl butyral (PVB) interlayers under short-term lateral loading (e.g. wind loads) would be similar to ordinary float glass of the same nominal thickness at the room temperature or below that. It was also suggested that the temperature at which the behavior changes is around 49°C. For long-term lateral loading (e.g. snow loads), the behavior of laminated glass is similar to ordinary float glass at temperatures of 0°C and below. Norville et al. [19] studied the behavior of laminated glass with different interlayer types and thicknesses under the effect of different heating rates. It was indicated that the strength of laminated glass increases as the interlayer thickness increases and decreases as the temperature increases. The available studies suggest that the behavior of laminated glass panels during fire exposure is closer to the extreme lower bound where the interlayer effect can be ignored. In this case, glass panes can expand freely depending on their temperature. In such a case, Eqs. 4-4a and 4-4b can be used for each glass panel separately to determine the self-induced stresses resulting from the thermal mismatch between the glass center and edge.

4.3 Validation

Wang and Hu [15] developed a validated ABAQUS mechanical model that can be used to determine the thermal stresses generated in laminated glass panels exposed to a fire. The glass panels and PVB-interlayer were modeled using 8-node-3D brick elements (C3D8 type from Abaqus library) with a total elements number of 25,200. The results of their model were used to validate the proposed method for determining the thermal stresses. The temperature of the glass is shown in Fig. 4-8 and the material properties were provided in Table 4-1. Fig. 4-10 shows that the results by Wang and Hu [15] closely matches the results of the simplified method, which assumes flexible interlayer. The results confirm that the PVB-interlayer has minor effect on the behaviour of the laminated glass assembly during fire exposure.

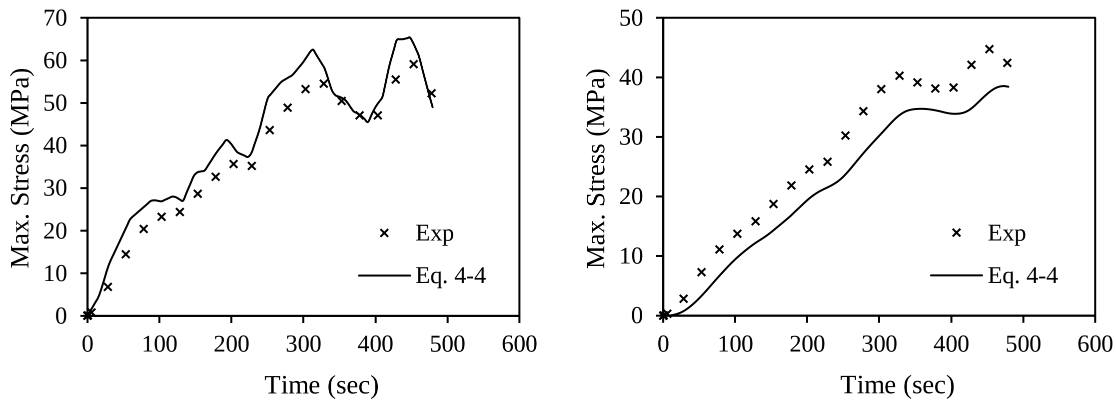

(a) Stress in Panel 1 (b) Stress in Panel 2

Figure 4-9: Validation of the proposed approach

4.4 Conclusion

This chapter provides a simple yet reliable approach to assess the behavior of laminated glass panels during fire exposure. A set of simplified methods were developed to conduct both heat transfer and stress calculations.

For heat transfer calculations, a simplified method proposed previously by the authors to estimate the temperature at the middle of the exposed part of ordinary glass thickness is adopted to calculate the average temperature of the interlayer. Finite element analysis is then utilized to develop an equation that can predict the temperature distribution across the thickness of the laminated glass panel.

For stress calculations, a simplified method to estimate the self-induced thermal strains, which maintain the plane section assumption, is developed. The development is made for the two extreme cases of rigid and flexible interface.

Predictions of the proposed approach were validated using data from the literature. The proposed approach was found to accurately predict the maximum thermal tensile stresses, developed during fire exposure. The results have also confirmed that the PVB-interlayer has minor effect on the behaviour of the laminated glass assembly during fire exposure.

4.5 References

[1] H.W. Emmons, The needed fire science, in: Fire Safety Science First International Symposium, IAFSS, 1986: pp. 33–53.

[2] R.T. Kuehnen, M.A. Youssef, Equivalent Standard Fire Duration to Evaluate Internal Temperatures in Natural Fire Exposed RC Beams, Fire Saf. J. 108 (2019) 102831. doi:10.1016/j.firesaf.2019.102831.

[3] R.T. Kuehnen, M.A. Youssef, Performance-Based Design of RC Columns using an Equivalent Standard Fire, Fire Safety Journal 111 (2020) 102935. doi:10.1016/j.firesaf.2019.102935.

[4] S.F. El-Fitiany, M.A. Youssef, Fire performance of reinforced concrete frames using sectional analysis, Engineering Structures. 142 (2017) 165–181. doi:10.1016/j.engstruct.2017.03.065.

[5] X.H. Dai, Y.C. Wang, C.G. Bailey, Numerical modelling of structural fire behaviour of restrained steel beam-column assemblies using typical joint types, Engineering Structures. 32 (2010) 2337–2351. doi:10.1016/j.engstruct.2010.04.009.

[6] H. Fang, M.B. Wong, Y. Bai, Heating rate effect on the thermophysical properties of steel in fire, J. Constr. Steel Res. 128 (2017) 611–617. doi:10.1016/j.jcsr.2016.09.016.

[7] O. Keski-rahkonen, Breaking of Window Glass Close, Fire Technology 12 (1988) 61–69.

[8] P.J. Pagni, Thermal glass breakage, Fire Safety Science (2003) 3–22. doi:10.3801/IAFSS.FSS.7-3.

[9] M. Haldimann, A. Luible, M. Overend, Structural use of glass, International Association for Bridge and Structural Engineering, Zürich, Switzerland, 2008.

[10] C. Bedon, M. Kozłowski, D. Honfi, Thermal assessment of glass façade panels under radiant heating: Experimental and preliminary numerical studies, J. Facade Des. Eng. 6 (2018) 049–064. doi:10.7480/jfde.2018.3.2477.

[11] M. Debuyser, J. Sjöström, D. Lange, D. Honfi, D. Sonck, J. Belis, Behaviour of monolithic and laminated glass exposed to radiant heating, Construction and Building Materials 130 (2017) 212–229. doi:10.1016/j.conbuildmat.2016.09.139.

[12] C. Bedon, Structural Glass Systems under Fire: Overview of Design Issues, Experimental Research, and Developments, Adv. Civ. Eng. 2017 (2017). doi:10.1155/2017/2120570.

[13] L. Galuppi, G. Royer-Carfagni, The post-breakage response of laminated heat-treated glass under in plane and out of plane loading, Compos. Part B Eng. 147 (2018) 227–239. doi:10.1016/j.compositesb.2018.04.005.

[14] A. Sabsabi, M.A. Youssef, S.F. El-Fitiany, A. Vedrtnam, Simplified Structural Analysis of Ordinary Glass Panels during Fire Exposure (Manuscript submitted for publication), Fire Safety Journal (2020).

[15] Y. Wang, J. Hu, Performance of laminated glazing under fire conditions, Compos. Struct. 223 (2019). doi:10.1016/j.compstruct.2019.110903.

[16] Dassault Systemes Simulia, Abaqus 6.14 documentation, Provid. Rhode Island, US. (2017).

[17] International Organization for Standards, ISO 834 - Fire Resistance Tests – Elements of Building Construction, Geneva, Switzerland, 2014.

[18] R.A. Behr, J.E. Minor, H.S. Norville, Structural behavior of architectural laminated glass, Journal of Structural Engineering 119 (1993) 202–222.

[19] H.S. Norville, K.W. King, J.L. Swofford, Behavior and strength of laminated glass, J. Eng. Mech. 124 (1998) 46–53.

Chapter 5

5 Summary and Conclusions

Glass breaking during fire exposure can have a significant impact on the severity of the event. The growing interest in using glass elements in different applications in the construction industry raises the need for reliable methods to assess their behavior in fire events. This thesis presented simple, practical, and rational methods to evaluate the behavior of ordinary and laminated glass panels during fire exposure. The proposed methods allow approximating the temperature gradients and the corresponding thermal stresses in glass panels exposed to fire events. The methods have been validated using existing experimental and finite element results. This chapter summarizes the work completed in each chapter of this thesis, highlights the important conclusions for each of the chapters, and provides the author's recommendations for future work.

5.1 Literature Review

This chapter summarizes the state-of-the-art literature and provides the needed background information on the topic. The chapter covered the following points:

- A brief explanation of the production process and the chemical composition of modern glass was provided.
- Glass products and their behavior were listed.
- Several key factors that affect the behavior of glass during fire exposure were identified. These factors include the type of glass, type of interlayer, glass panel dimensions, edge finishing, temperature gradients, imposed heat flux, environmental conditions, and the edge restrains.

5.2 Simplified Structural Analysis of Ordinary Glass Panels during Fire Exposure

A simple yet reliable approach to assess the behavior of ordinary glass panels during fire exposure was provided. A set of simplified methods were developed to conduct both heat transfer and stress calculations. For heat transfer calculations, a simplified method to estimate the temperature at the center of the glass panel was proposed. The method assumes that the temperature across the glass thickness is constant. The finite element method was then utilized to develop an equation that relates the temperature at the edge of the panel to the temperature at its center. For stress calculations, a simplified method to estimate the self-induced thermal strains, which maintain the plane section assumption, is developed considering cases of uniform fire exposure and non-uniform fire exposure. Predictions of the proposed approach were compared to the experimental and numerical work by others. The comparisons have confirmed the accuracy of the proposed approach in estimating the maximum tensile stress developed during fire exposure.

5.3 Simplified Structural Analysis of Laminated Glass Panels during Fire Exposure

This chapter provides a simple yet reliable approach to assess the behavior of laminated glass panels during fire exposure. A set of simplified methods were developed to conduct both heat transfer and stress calculations. For heat transfer calculations, a simplified method proposed previously by the authors to estimate the temperature at the middle of the exposed part of ordinary glass thickness is adopted to calculate the average temperature of the interlayer. Finite element analysis is then utilized to develop an equation that can predict the temperature distribution across the thickness of the laminated glass panel. For stress calculations, a simplified method to estimate the self-induced thermal strains, which maintain the plane section assumption, is developed. The development is made for the two extreme cases of rigid and flexible interface. Predictions of the proposed approach were validated using data from the literature. The proposed approach was found to accurately predict the maximum thermal tensile stresses, developed during fire exposure. The results have also confirmed that the PVB-interlayer has minor effect on the behaviour of the laminated glass assembly during fire exposure.

5.4 Thesis Limitations

The followings are the limitations of the work done in this thesis:

- The temperature distribution in the planar direction was simplified as a one-dimensional temperature distribution at the exposed part and uniform at the covered part. The covered part was assumed completely protected from radiation and convection heating from fire.

- Given the limited available experimental work on laminated glass behavior during fire exposure, the proposed method needs to be further validated with a broader range of fire exposures.

- The proposed method for heat transfer calculation in laminated glass exposed to fire is valid for laminated glass panels consisting of two glass panels connected with one PVB interlayer.

5.5 Recommendation for future research

The work presented in this thesis discusses the effect of fire exposure on ordinary and laminated glass sections. For the future development and improvement of the research, the following recommendations can be made:

1. Experimental testing is needed to further validate the proposed methods with broader range of fire exposures.
2. The proposed methods need to be extended to be applicable to other types of glass such as heat-treated glass panels.
3. Expand on the proposed methods to differentiate between the time of first crack and the time of glass fallout.

Curriculum Vitae

Name:	Amer Sabsabi
Post-secondary Education and Degrees:	Jordan University of Science and Technology Irbid, Jordan 2012-2017 B.E.Sc. The University of Western Ontario London, Ontario, Canada 2018-2020 M.E.Sc.
Honours and Awards:	Peter A. Rosati Award for Outstanding Teaching in the Civil and Environmental Engineering Department 2019
Related Work Experience	Teaching Assistant The University of Western Ontario 2019-2020

Publications:

A. Sabsabi, M.A. Youssef, S.F. El-Fitiany, and A. Vedrtnam. "Improving Fire Safety of Structures Through the Development of Fire-Retardant Laminated Glass Glazing." Presentation at the 7th Annual IC-IMPACTS Research Conference, Vancouver, BC, June 2019.

A. Sabsabi, M.A. Youssef, S.F. El-Fitiany, and A. Vedrtnam. "Simplified Structural Analysis of Ordinary Glass Panels during Fire Exposure." Fire Safety Journal. Manuscript submitted for publication, July 2020.

A. Sabsabi, M.A. Youssef, S.F. El-Fitiany, and A. Vedrtnam. "Simplified Structural Analysis of Laminated Glass Panels during Fire Exposure." Fire Safety Journal. Manuscript to be submitted for publication, August 2020.

A. Vedrtnam, C. Bedon, M.A. Youssef, M. Wamiq, A. Sabsabi, S. Chaturvedi, Experimental and numerical structural assessment of transparent and tinted glass during fire exposure, Construction and Building Materials 250 (2020). doi:10.1016/j.conbuildmat.2020.118918.